Design and Analysis of Hierarchical Physical Layer Network Coding

Haoyuan Zhang, *Student Member, IEEE*, Lei Zheng, *Student Member, IEEE*, and Lin Cai, *Senior Member, IEEE*

***Abstract*— This paper proposes a new relaying technique, hierarchical physical layer network coding (H-PNC), aimed at increasing the spectrum and energy efficiency in multi-hop wireless networks by supporting two bi-directional traffic flows simultaneously. H-PNC is applicable to the scenario in which two source nodes exchange data with the help of a relay, and the relay also needs to exchange data with one source node in an asymmetric two-way relay channel network, where the channel conditions of two source-relay links are asymmetric. H-PNC arranges transmissions in two stages, the multiple access (MA) stage and the broadcast (BC) stage. In the MA stage, the source node with the better channel to the relay can superimpose the symbol targeting to the relay on the symbol targeting to the other source node. In the BC stage, the relay can superimpose the symbol targeting to the source node with the better channel on the broadcast symbol. Thus, one more bidirectional information exchange is achieved beyond traditional PNC. Designs and optimizations of three H-PNC schemes are presented, and the error performance of QPSK–BPSK H-PNC is derived. Extensive simulations have been conducted to evaluate the system performance. Both theoretical analysis and simulation results demonstrated that H-PNC achieves a substantial performance gain.**

***Index Terms*— Physical layer network coding, hierarchical modulation, two way relay channel.**

I. Introduction

PHYSICAL layer network coding (PNC) was proposed in [2] and [3] to improve the throughput of wireless multi-hop networks. The majority of PNC research were studied under the two-way relay channel (TWRC) scenario, where bi-directional information exchange between two source nodes can be achieved assisted by a relay node, when the source nodes are out of each other's transmission range. The key idea of PNC is to enable the source nodes to transmit signals to the relay simultaneously in the multiple access (MA) stage, and allow the signals from the two sources being superimposed at the relay. The network-coded symbols, which contain the necessary information of the source signals, are constructed from the superimposed signals and broadcast back to the source nodes in the broadcast (BC) stage. The concurrent transmission achieves a higher spectrum efficiency [2]–[4].

Since PNC was proposed, most of the previous research considered the symmetric TWRC scenario, where two source-relay links have similar channel conditions. Thus, the same channel coding and modulation schemes can be applied by the sources, and an equivalent data exchange ratio can be achieved [5]–[15]. However, in a more general asymmetric TWRC scenario, when the two source-relay links have different channel qualities or an unequal data exchange is required between the sources, different modulations (and coding) may be selected by the two source nodes. The relay operations designed for the symmetric TWRC may achieve a low spectrum efficiency under asymmetric TWRC scenarios and need to be reconstructed by heterogeneous modulation PNC designs [16]–[23].

Although the heterogeneous modulation PNC schemes try to maximize the system throughput under the asymmetric TWRC scenario, the system throughput is subject to the channel of the bottleneck link [24]–[26]. In an asymmetric TWRC scenario, to guarantee a BER threshold, the relay may need to decrease the network-coded symbol from a higher-order modulation into a lower-order modulation and broadcast in multiple slots, and in each slot the channel of the source-relay link with the better channel quality is not fully utilized by only broadcasting a lower-order modulation symbol. For example, consider QPSK-BPSK heterogeneous modulation PNC, where sources A and B use QPSK and BPSK in the MA stage, respectively, determined by the source-relay channel conditions. The network-coded symbol obtained at the relay is a QPSK symbol subject to the Latin square constraint [6]. Heterogeneous modulation PNC designs benefit from the asymmetric data exchange ratio between sources A and B, e.g., 2:1 for QPSK-BPSK heterogeneous modulation PNC. However, since the bottleneck link between source B and relay R can only support BPSK in the BC stage, the QPSK network-coded symbol needs two slots to be broadcast back to the sources. Thus, the overall throughput of the system is 1 bit/slot, which is the same as that of the symmetric BPSK-BPSK PNC.

Thus, it is worthy to develop new schemes that can fully utilize the channel of the source-relay link with the better channel condition. Also, the majority of the previous PNC research considered the scenarios that only one bidirectional information exchange between two sources can be achieved with the help of a relay [2]–[23], or in a multiple access scenario [27]. In the scenarios that the relay also needs to

Manuscript received October 31, 2016; revised March 13, 2017 and June 28, 2017; accepted September 10, 2017. Date of publication September 26, 2017; date of current version December 8, 2017. This paper was presented at the IEEE ICC, London, U.K., June 2015 [1]. The associate editor coordinating the review of this paper and approving it for publication was C. Tepedelenlioglu. *(Corresponding author: Lin Cai.)*

The authors are with the Department of Electrical and Computer Engineering, University of Victoria, Victoria, BC V8P 5C2, Canada (e-mail: hyuan@uvic.ca; zhengl@uvic.ca; cai@uvic.ca).

Color versions of one or more of the figures in this paper are available online at http://ieeexplore.ieee.org.

Digital Object Identifier 10.1109/TWC.2017.2755017

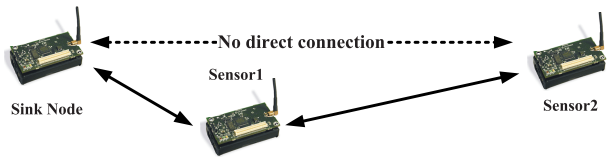

Fig. 1. Motivating example.

exchange information with the source node, the traditional PNC solutions [5]–[15] including heterogeneous modulation PNC [16]–[23] are far from optimal. The above two reasons motivate us to develop new PNC solutions to new scenarios. This scenario occurs in various multi-hop networks, either infrastructure-based or *ad hoc* networks. For instance, in a sensor network as shown in Fig. 1, the sink node may need to exchange data with two sensor nodes, and the sensor1 can act as the relay for the sensor2 who is far away from the sink.

H-PNC arranges transmissions in two stages: multiple access (MA) stage and broadcast (BC) stage. In the MA stage, the source node with the better source-relay channel quality can superimpose the symbol targeting to the relay on the symbol targeting to the other source node. In the BC stage, the relay can superimpose the symbol targeting to the source node (with the better source-relay channel quality) on the broadcast symbol. Under the asymmetric TWRC scenario, where sources A and B support QPSK and BPSK, respectively, the proposed QPSK-BPSK hierarchical physical layer network coding (H-PNC) achieves 1 bit/slot data exchange between sources A and B and additional 1 bit/slot data exchange between source A and relay R.[1] Also only one slot is needed for the broadcast stage as the symbol from relay R to source A is superimposed on the BPSK network-coded symbol achieved by hierarchical modulation design. Thus, the system throughput is 2 bits/slot, which outperforms the 1 bit/slot throughput of QPSK-BPSK heterogeneous modulation PNC and symmetric BPSK-BPSK PNC. One more bidirectional information exchange beyond PNC can be achieved by taking advantage of the channel of the source-relay link with the better channel condition.

H-PNC design is more challenging than the traditional PNC. First, different from PNC, where the superimposed signals can be directly mapped to a network-coded symbol; in H-PNC, the symbol transmitted from the source targeted to the relay should be extracted from the superimposed symbols first, and then the remaining superimposed symbols are mapped to a network-coded symbol. Thus, the error performance of H-PNC is more sensitive to the superimposed constellation at the relay in the MA stage. Second, in H-PNC, hierarchical constellation should be designed for both the transmit constellation in the MA stage and the broadcast constellation in the BC stage, where both the bit-symbol labeling and constellation structures should be optimized. Third, the mapping functions applied by PNC and H-PNC relays need to satisfy the Latin square constraint [6], and adaptive mapping [5] can still be applied in certain modulation combinations of H-PNC. However, new design criteria and constraints are needed for H-PNC due to the additional bidirectional information exchange.

The main contributions of this paper are three-fold. First, a new transmission solution, H-PNC, is proposed, which achieves the data exchange not only between two source nodes, but also between the relay and the source node with the better channel. H-PNC outperforms the traditional heterogeneous modulation PNC and symmetric PNC solutions in terms of the system throughput by fully utilizing the channel of the source-relay links. Second, three H-PNC sample designs are presented, and the design and optimization criteria are investigated. The design of H-PNC should jointly consider the optimization of bit-symbol labeling, hierarchical modulation constellation design and H-PNC mapping constraint. Third, we develop an analytical framework to derive the error performance of QPSK-BPSK H-PNC under both AWGN and Rayleigh fading channels. Extensive simulations have been conducted to study the BER performance of H-PNC under both AWGN and Rayleigh fading channels, and the throughput and throughput upper bound performance of H-PNC are studied and compared with the traditional PNC.

The rest of this paper is organized as follows. Section II introduces the related work. Section III introduces the system model and H-PNC procedure. Section IV presents the detailed designs and optimizations of three H-PNC samples. Section V derives the error performance of QPSK-BPSK H-PNC. Performance evaluations are presented in Section VI, followed by the concluding remarks in Section VII.

II. Related Work

PNC was proposed by Zhang *et al.* [2] and Popovski and Yomo [3], independently, in 2006 inspired by network coding [28], [29]. Most of the existing work was researched in the symmetric TWRC network [5]–[9], [11]–[13], [15], where two source-relay links have similar channel conditions. Thus, the same coding and modulation schemes are used by the two sources and an equal data exchange rate can be achieved. The authors in [5] investigated that the optimal mapping function varies with two source-relay channel conditions, and proposed the adaptive mapping design. The authors in [6] found out that the mapping function design should follow the Latin square constraint. PNC performance was compared with the traditional network coding and TDMA schemes in [7], and a non-binary PNC scheme was proposed in [8]. The authors in [9]–[14] studied how to integrate the channel coding into PNC schemes under the symmetric TWRC scenario. The authors in [15] considered a generalized symmetric PNC scenario with one relay and arbitrary number of sources. The authors in [30] and [31] studied the achievable rates in the two-path relay channel (TPRC), where the objective is to transmit the information from one source to one destination aided by two half-duplex relays instead of the information exchange between two sources.

Later on, it was found that under the asymmetric TWRC scenario, where two source-relay links have quite different channel conditions, the traditional symmetric PNC design cannot be directly applied or otherwise results in a low spectrum efficiency due to the bottleneck source-relay link,

[1] If relay R has data exchange requirement with source B instead of source A, H-PNC cannot be applied and other time-division scheduling should be applied.

and also symmetric PNC design is unsuitable to support the asymmetric data exchange requirement [16]–[20], [23]. In [16], the impact of the source-relay channels on PNC was studied, which demonstrated that the bottleneck link has a large impact on the PNC error performance under asymmetric TWRC. In [17], adaptive modulation and network coding (AMNC) was proposed under the assumption that the carrier-phase synchronization can be achieved at the relay. The authors in [18] and [19] proposed and studied the decode-and-forward joint-modulation (DF-JM) scheme, where a higher-order modulation network-coded symbol is designed by directly combining the two source symbols. However, a higher-order network-coded symbol reduces the system throughput as more broadcast slots are needed in the BC stage subject to the bottleneck link. The authors in [20]–[22] proposed PNC without increasing the modulation order of the network-coded symbol, and the authors in [21] and [22] further studied the adaptive mapping function design considering the impact of carrier-phase. The authors in [27] proposed a network-coded multiple access (NCMA) model, which combines the PNC and multiuser decoding (MUD). The target is to deliver the information from one source to other node instead of the simultaneously transmit source. The authors in [23] studied various subtleties of applying linear PNC with q-level pulse amplitude modulation (q-PAM) under asymmetric TWRC to achieve the imbalanced data between two sources, and the error performance of q-PAM based symmetric PNC under Rayleigh fading channels was studied in [32].

Although the above proposed PNC designs under asymmetric TWRC targeted to support the unequal data exchange ratio and tried to maximize the system throughput, the overall throughput (bits per slot) taking both sources into account is still limited by the bottleneck link, also the channel of the source-relay link with the better channel condition is not fully utilized by broadcasting a lower-order modulation symbol determined by the bottleneck link. How to fully utilize the channel of the source-relay link with the better channel condition while achieving the information exchange between multiple sources is our main target in this work. The hierarchical constellation designs in [33]–[35] under non-PNC scenario provided guidelines for the H-PNC constellation designs in this work.

III. System Model and H-PNC Procedure

Consider an asymmetric TWRC scenario with two source nodes A and B, and the relay node R. Without loss of generality, we assume that the channel condition between source A and relay R (L_{ar}) is better than that between source B and relay R (L_{br}). Sources A and B need to exchange information with the help of relay R because they are out of each other's transmission range. Meanwhile, source A also needs to exchange information with relay R. We assume perfect channel estimations at the receivers only. Symbol-level synchronization is assumed at the relay, and the feasibility of the symbol-level synchronization has been studied in [36] and [37]. Note that, the carrier-phase synchronization is not required at the relay in the H-PNC application. Throughout this paper, the H-PNC design is only considered in a symbol-level, i.e., only end-to-end channel coding can be combined. How to integrate the channel error coding into H-PNC schemes in a link-to-link coding is beyond the scope of this work.

Let $\mathcal{M}_m$ be 2^mQAM/PSK modulation with modulation order m. m_a and m_b are the modulation orders for the transmissions from sources A and B, respectively. One symbol transmitted from source A, S_a, consists of two sub-symbols: a symbol targeting to relay R, S_{ar}, and a symbol targeting to source B, S_{ab}, i.e., $S_a = [S_{ar}, S_{ab}]$, where $[,]$ denotes that sub-symbols S_{ar} and S_{ab} are concatenated to compose one symbol S_a. Denote S_{ba} as the symbol transmitted from source B targeting to source A. Let $\mathbb{Z}_{2^m}$ be a non-negative integer set, where $\mathbb{Z}_{2^m} = \{0, 1, \ldots, 2^m - 1\}$, and we have $S_a \in \mathbb{Z}_{2^{m_a}}$, $S_{ba} \in \mathbb{Z}_{2^{m_b}}$. Note that each integer in $\mathbb{Z}_{2^m}$ can be expressed by an m-bit symbol. Throughout this paper, SNR is defined as the received symbol energy to noise ratio. For Rayleigh fading channels, SNR is the average received SNR.

A. H-PNC Procedure

H-PNC takes two stages, the multiple access (MA) stage and the broadcast (BC) stage, to achieve two bidirectional information exchange, i.e., between both source A and relay R, and sources A and B. The H-PNC procedure is introduced as follows.

1) Multiple Access Stage: In the MA stage, both sources A and B transmit symbols to relay R simultaneously. The transmitted symbols are $X_a = \mathcal{M}_{m_a}(S_a)$ and $X_b = \mathcal{M}_{m_b}(S_{ba})$. The received signals at relay R are $Y_r = H_a X_a + H_b X_b + N_r$, where H_a and H_b are the channel gains of links L_{ar} and L_{br}, respectively, and N_r is the Gaussian noise with a variance of $2\sigma^2$. Denote $H_b/H_a = \gamma \exp(j\theta)$, where γ is the amplitude ratio and θ is the phase shift difference with uniform distribution in $[0, 2\pi)$.

Denote (S_a, S_{ba}) as a symbol pair, i.e., two symbols S_a and S_{ba} from the two source nodes are superimposed at relay R. One symbol pair (S_a, S_{ba}) is mapped to a unique constellation point at relay R, which can be expressed as

$$H_a \mathcal{M}_{m_a}(s_1) + H_b \mathcal{M}_{m_b}(s_2), \quad \text{for all } s_1 \in \mathbb{Z}_{2^{m_a}},\ s_2 \in \mathbb{Z}_{2^{m_b}}. \tag{1}$$

The maximum likelihood (ML) detection is used to jointly decode symbols S_a and S_{ba} from Y_r. Denote the estimation of (S_a, S_{ba}) by $(\hat{S}_a, \hat{S}_{ba})$, we have

$$(\hat{S}_a, \hat{S}_{ba}) = \underset{(s_1,s_2)\in\mathbb{Z}_{2^{m_a}}\times\mathbb{Z}_{2^{m_b}}}{\operatorname{argmin}} \left|Y_r - H_a \mathcal{M}_{m_a}(s_1) - H_b \mathcal{M}_{m_b}(s_2)\right|^2. \tag{2}$$

$\hat{S}_a$ consists of the estimations of both S_{ar} and S_{ab}, i.e., $\hat{S}_a = [\hat{S}_{ar}, \hat{S}_{ab}]$. The information transmission from source A to relay R is achieved by extracting $\hat{S}_{ar}$ from $\hat{S}_a$. Then relay R uses a mapping function $\mathcal{C}$ to map the left symbol pair $(\hat{S}_{ab}, \hat{S}_{ba})$ to a network-coded symbol $S_n = \mathcal{C}(\hat{S}_{ab}, \hat{S}_{ba})$. We have $S_n \in \mathbb{Z}_{2^{\max(m_{ab},\ m_b)}}$ subject to the Latin square constraint, where m_{ab} is the modulation order for the sub-symbol S_{ab}. The mapping function $\mathcal{C}$ is known by

all nodes. Its design is a key issue and will be discussed in Subsections III-B and C, and Section IV.

2) Broadcast Stage: In the BC stage, the information transmission from relay R to source A, S_{ra}, can be achieved by superimposing S_{ra} onto the network coded symbol S_n on a hierarchical modulation constellation [33]–[35]. S_n is modulated in the base layer to try to successfully broadcast S_n in the BC stage, and S_{ra} is modulated in the enhancement layer to fully utilize the channel of source-relay link L_{ar}. The broadcast symbol by relay R in the BC stage is $S_r = [S_n, S_{ra}]$. Finally, at source A, S_r is estimated by ML detection, i.e., $\hat{S}_r = [\hat{S}_n, \hat{S}_{ra}]$, and the information from relay R to source A is obtained from $\hat{S}_{ra}$, and that from source B to source A, S_{ba}, is obtained from $\hat{S}_n$ together with the original transmitted symbol S_{ab} and the mapping function $\mathcal{C}$ used at relay R [1], [20]. At source B, only the base layer symbol S_n is estimated, and S_{ab} is obtained in a similar way.

Note that, subject to the bottleneck link L_{br}, only a modulation order m_b can be supported given a BER threshold. When the modulation order of S_n, $\max(m_{ab}, m_b)$, is larger than m_b, relay R uses $\lceil \frac{m_{ab}}{m_b} \rceil$ slots to broadcast S_n to guarantee that in each BC slot the modulation order of the base layer is no larger than m_b. An example of this case is 8QAM-BPSK H-PNC case 2, which will be discussed in Subsection IV-C.

In the initialization of H-PNC, the data amount to be exchanged between A, B and R should be collected, and the relay R estimates two source-relay channel conditions and determines the modulations applied by the sources by jointly considering two source-relay channel conditions and the data exchange requirements, and sends the modulation configuration to the sources.

B. Mapping Function $\mathcal{C}$

The optimal mapping functions vary with the two source-relay channel conditions [5], [21], [22]. Adaptive mapping is a mapping function design method, in which the relay dynamically selects a mapping function $\mathcal{C}$ according to the two source-relay channel conditions. The relay needs to inform the sources the mapping functions applied, where the frequency is determined by the dynamic of the source-relay channels. Denote the error probability that $S_n \neq \mathcal{C}(S_{ab}, S_{ba})$ as relay mapping error rate, BER_r. Adaptive mapping design aims to minimize BER_r by the closest-neighbour clustering algorithm. We refer the readers to [5], [21], and [22] for the adaptive mapping designs for symmetric and asymmetric PNC, respectively.

For 2^{m_1}QAM/PSK-2^{m_2}QAM/PSK H-PNC, where m_1 and m_2 denote two integers, adaptive mapping can be applied as long as either S_{ab} or S_{ba} contains more than one bit; otherwise, exclusive or (XOR) is the unique mapping method. For example, as discussed in Subsection IV-C, for QPSK-BPSK H-PNC and 8QAM-BPSK H-PNC case 1 (S_{ab} contains 1 bit), XOR mapping is the unique mapping method; for 8QAM-BPSK H-PNC case 2 (S_{ab} contains 2 bits), adaptive mapping functions can be designed.

C. Mapping Constraints

H-PNC mapping function $\mathcal{C}$ design is more challenging compared to the traditional PNC. The H-PNC mapping function $\mathcal{C}$ design subjects to two constraints: one is the Latin square constraint [6] expressed in (3), also known as the exclusive law [5]; the other one is the H-PNC constraint expressed in (4).

$$\begin{aligned} &\mathcal{C}(s_1,\ s_2) \neq \mathcal{C}(s_1',\ s_2) \text{ for any } s_1 \neq s_1' \in \mathbb{Z}_{2^{m_{ab}}} \\ &\qquad\qquad \text{and } s_2 \in \mathbb{Z}_{2^{m_b}}; \\ &\mathcal{C}(s_1,\ s_2) \neq \mathcal{C}(s_1,\ s_2') \text{ for any } s_2 \neq s_2' \in \mathbb{Z}_{2^{m_b}} \\ &\qquad\qquad \text{and } s_1 \in \mathbb{Z}_{2^{m_{ab}}}. \end{aligned} \tag{3}$$

$$\begin{aligned} &\mathcal{C}([s_1,\ s_2], s_3) = \mathcal{C}([s_1',\ s_2], s_3) \text{ for any } s_1 \neq s_1' \in \mathbb{Z}_{2^{m_{ar}}}, \\ &\qquad s_2 \in \mathbb{Z}_{2^{m_{ab}}} \text{ and } s_3 \in \mathbb{Z}_{2^{m_b}}. \end{aligned} \tag{4}$$

The Latin square constraint implies that the minimum modulation order of the network-coded symbol S_n is $\max(m_{ab}, m_b)$. The H-PNC constraint implies that, in the expected received constellation map at the relay, given s_a and s_{ba}, $s_a \in \mathbb{Z}_{2^{m_a}}$ and $s_{ba} \in \mathbb{Z}_{2^{m_b}}$, the symbol pair (s_a, s_{ba}) only appears once; however, sub-symbol pair (s_{ab}, s_{ba}), $s_{ab} \in \mathbb{Z}_{2^{m_{ab}}}$, appears $2^{m_{ar}}$ times, where m_{ar} is the modulation order of sub-symbol S_{ar}. All the same sub-symbol pairs (s_{ab}, s_{ba}) should be mapped to the same network-coded symbol S_n.

We use an example to illustrate the H-PNC constraint. Consider QPSK-BPSK H-PNC, where $S_a = [S_{ar}, S_{ab}]$ is a QPSK symbol, and S_{ba} is a BPSK symbol. Two sub-symbol pairs (S_{ab}, S_{ba}) equal to $(0, 1)$ and $(1, 0)$, belong to $([0, 0], 1)$ and $([0, 1], 0)$, respectively, may be both mapped to a network-coded symbol $S_r = \mathcal{C}'(S_{ab}, S_{ba}) = 1$ by a mapping function $\mathcal{C}'$. By the H-PNC constraint, the mapping function $\mathcal{C}'$ further determines that other two sub-symbol pairs, i.e., $(0, 1)$ and $(1, 0)$ belong to $([1, 0], 1)$ and $([1, 1], 0)$, respectively, should also be mapped to the same network-coded symbol $S_r = 1$ by the mapping function $\mathcal{C}'$. The Latin square and H-PNC constraints have important impact on the H-PNC design, which will be discussed in Section IV.

IV. H-PNC Sample Design

In this section, we first present the QPSK-BPSK H-PNC design in details starting with an illustrative example. Then we present higher-order modulation H-PNC designs, including two cases of 8QAM-BPSK H-PNC. The design and optimization criteria are presented.

A. QPSK-BPSK H-PNC Example

We first give an example to illustrate how H-PNC works in a nutshell in Fig. 2. Fig. 2(a) shows an example of QPSK-BPSK H-PNC procedure, where source A exchanges one unit of data with source B and relay R each. In the MA stage, source A transmits bit $S_{ar} = 0$ (targeting to relay R) and bit $S_{ab} = 1$ (targeting to source B) using a QPSK symbol $S_a = [S_{ar}, S_{ab}] = 01$. Source B transmits symbol $S_{ba} = 0$ (targeting to source A) by BPSK. Suppose relay R successfully demodulates the symbol pair $(\hat{S}_a, \hat{S}_{ba}) = (01, 0)$ by ML detection, and obtains $\hat{S}_{ar} = 0$ from source A by extracting $\hat{S}_{ar}$ from $\hat{S}_a$. Then relay R applies the mapping function $\mathcal{C}$ (For QPSK-BPSK H-PNC, mapping function $\mathcal{C}$ is XOR uniquely) to map $(\hat{S}_{ab}, \hat{S}_{ba})$ to a network-coded symbol $S_n = \mathcal{C}(\hat{S}_{ab}, \hat{S}_{ba}) = 1$ XOR $0 = 1$. In the BC stage,

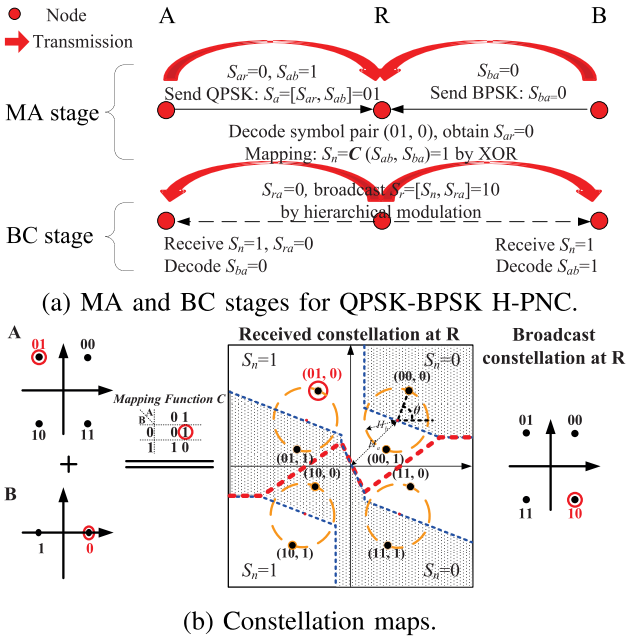

Fig. 2. QPSK-BPSK H-PNC with $\gamma = 0.5$ and $\theta = \frac{3\pi}{8}$.

relay R targets to transmit one unit of data $S_{ra} = 0$ to source A, which is superimposed on the network-coded symbol $S_n = 1$ using a hierarchical constellation. S_n is positioned on the base layer, and S_{ra} is positioned on the enhancement layer. Thus, relay R broadcasts $S_r = [S_n, S_{ra}] = 10$. Finally, source A receives and obtains the estimations of both $\hat{S}_n = 1$ and $\hat{S}_{ra} = 0$ by ML detection. As source A already knows $S_{ab} = 1$, and thus $S_{ba} = 0$ can be derived by applying the mapping function $\mathcal{C}$ (XOR) conversely. Source B only needs to demodulate $\hat{S}_n = 1$, and obtains $S_{ab} = 1$ in a similar way.

Fig. 2(b) shows the constellation maps of QPSK-BPSK H-PNC. The left two constellations show the transmit constellations at sources A and B, respectively. The right constellation shows the broadcast constellation at relay R in the BC stage. Note that, although both the transmit constellations applied at source A and the broadcast constellation at relay R use the 2/4-QAM hierarchical constellation design, the bit-symbol labelings are different. The explanation will be discussed in Subsection IV-B. The middle figure shows the expected received constellation map at relay R. The red dotted curves define the decision boundaries for S_{ar}, and the blue curves define those for S_n. The shadowed regions are the decision regions of $S_n = 0$. The four dashed circles are formed by the BPSK symbols, $H_b\mathcal{M}_1(S_{ba})$, shifted by θ and superimposed to the QPSK symbols $H_a\mathcal{M}_2(S_a)$, i.e., the center of each circle is $H_a\mathcal{M}_2(S_a)$.

We can observe that, the expected constellation at relay R in Fig. 2(b) is determined not only by $|H_a|$ and $|H_b|$, but also by the original transmission constellation at source A. Modifying the original transmit constellations at the sources would influence the structure of the expected received constellation map. For example, given the symbol energy, enlarging the Euclidean distance between symbols 00 and 11 on the transmitting constellation of source A would benefit the demodulation of

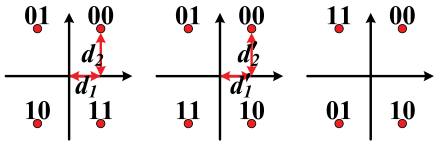

(a) Labeling-1. (b) Labeling-2. (c) Labeling-3.

Fig. 3. QPSK labeling methods and hierarchical QPSK constellation maps.

S_{ar} thanks to a larger Euclidean distance, but the probability of obtaining a correct $S_n = \mathcal{C}(S_{ab}, S_{ba})$ may be affected negatively as the distance of two BPSK circles horizontally would shrink. Another example is the symbol pairs $(01, 1)$ and $(10, 0)$ on the expected received constellation at relay R in Fig. 2(b). Individually demodulating each bit of them would cause a larger error probability as the Euclidean distance between them is relatively small. However, we only need to distinguish the first bit S_{ar} of the QPSK symbols, because after S_{ar} is extracted from S_a, $(01, 1)$ and $(10, 0)$ shrink to $(1, 1)$ and $(0, 0)$, and are both mapped to $S_n = 0$ by the XOR mapping. Thus, from the above examples, we can observe that the design and optimization of the transmit constellations at sources are extremely important. H-PNC design should jointly consider the transmit constellations and the positive effects of the mapping functions.

B. QPSK-BPSK H-PNC Constellations

In this subsection, the designs of the transmit constellation at source A in the MA stage, and the broadcast constellation at relay R in the BC stage will be studied, respectively. We observe that Gray mapping is not the optimal bit-symbol labeling for the transmit constellation of source A, and hierarchical modulation constellations should be designed for both constellations.

1) Transmit Constellation at Source A: Different from the broadcast constellation at relay R, the transmit constellation design at source A also needs to consider the impact of the superimposed signals on the received constellation map at relay R. Denote BER_{ar} as the bit error rate (BER) of S_{ar}. For the bit-symbol labeling of QPSK constellation, there are totally three methods to label the 2-bit symbols on the constellation map as shown in Figs. 3(a), 3(b) and 3(c), denoted as labeling-1, labeling-2 and labeling-3, respectively. For QPSK-BPSK H-PNC, labeling-1 is better than labeling-2, and labeling-2 is better than labeling-3 in terms of BER. The reasons are discussed in the following.

First, we compare labeling-2 and labeling-3. In the QPSK symbol, for the first bit S_{ar}, labeling-2 reduces the error probability in the horizontal direction, which can reduce BER_{ar}. For the second bit S_{ab}, given S_{ba}, labeling-2 and labeling-3 are mapped to the same S_n after S_{ar} is extracted from S_a, so they have the same BER_r performance. Thus, labeling-2 is better than labeling-3. Comparing labeling-1 and labeling-2, they have the same BER_{ar} performance. For the second bit S_{ab}, the impact of S_{ba} on the expected received constellation at relay R should be considered. One example of the worst-case is shown in Fig. 4, where $\theta = \frac{\pi}{2}$ and $\gamma = 0.5$.

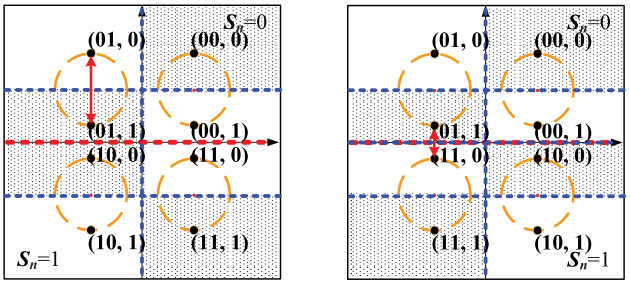

(a) Labeling-1. (b) Labeling-2.

Fig. 4. Worst case comparison of labeling-1 and labeling-2.

Note that $\theta = \frac{3\pi}{2}$ is another worst case of labeling-2. The red segment shows the smallest Euclidean distance between different constellation points. For labeling-2, the Euclidean distance between symbol pairs $(01, 1)$ and $(11, 0)$ is relatively small, and they are mapped to different S_n after extracting S_{ar}, i.e., $(01, 1)$ and $(11, 0)$ will be mapped to $\mathcal{C}(1, 1) = 0$ and $\mathcal{C}(1, 0) = 1$ by XOR, respectively, which leads to a higher BER_r. For labeling-1, $(01, 1)$ and $(10, 0)$ are both mapped to $S_n = 0$ by XOR after S_{ar} is extracted, and the smallest Euclidean distance for labeling-1 is always the diameter of BPSK circles whatever θ is. Therefore we have the conclusion that for the transmitting constellation at source A, labeling-1 is better than labeling-2, and labeling-2 is better than labeling-3 in terms of BER.

The above conclusion provides insights to design an appropriate H-PNC transmit constellation at source A. The bit-symbol labeling criterion is summarized as follows: for the symbol-set $S_a \in \mathbb{Z}_{2^{m_a}}$, $S_a = [S_{ar}, S_{ab}]$, symbols of S_a with the same S_{ar} should be grouped on the constellation to improve the BER_{ar} performance, and symbols of S_a with the same S_{ab} should be separated on the constellation to guarantee the BER_r performance. The BER_r performance further affects the final successful demodulation rate of S_{ab} and S_{ba} in the BC stage. Based on the above insights, labeling-1 is the optimal labeling scheme for the transmit constellation at source A and is adopted.

To have an optimal constellation design for H-PNC, an optimal bit-symbol labeling scheme is necessary but not sufficient. If labeling-1 is directly applied by source A with a symmetrical constellation, the BER_{ar} performance is much worse than that of BER_r because of the smallest Euclidean distance. Therefore, we propose to apply QPSK hierarchical modulation to further optimize the constellation map. Denote $\lambda_1 = \frac{d_2}{d_1}$ as shown in Fig. 3(a). Assume that all the symbols have unit energy $E_s = 1$, i.e., ${d_2}^2 + {d_1}^2 = 1$. It is easy to observe that enlarging d_2 reduces BER_{ar}. However, when $\lambda_1 = 1$, BER_r can be minimized thanks to the symmetrical features of the constellation maps. Therefore there is a tradeoff to set λ_1.

The optimal λ_1 is obtained by maximizing the overall successful transmission rate in the MA stage. For QPSK-BPSK H-PNC, it can be simplified as

$$\min_{\lambda_1} \; 2 \cdot \text{BER}_r + \text{BER}_{ar}, \tag{5}$$

where the coefficient 2 before BER_r denotes that one unit of BER_r error may cause two units of final decoding error, i.e., both S_{ab} and S_{ba} in the BC stage under the condition of the broadcast process in BC stage are successful. Note that the small probability that the network-coded symbol is erroneous but the end-to-end estimation at the BC stage is correct is neglected in (5) to simplify the analysis. The theoretical derivations of BER_r and BER_{ar} of QPSK-BPSK H-PNC will be studied in Section V.

2) Broadcast Constellation at Relay R: In the BC stage, relay R uses a hierarchical constellation to broadcast the superimposed symbol $S_r = [S_n, S_{ra}]$. For the bit-symbol labeling of the broadcast constellation, S_n is positioned on the base layer, and S_{ra} is positioned on the enhancement layer. It is easy to find that labeling-2 as shown in Fig. 3 is optimal. As to maximize the successful demodulation rate, i.e., to maximize the Euclidean distance between bits '0' and '1', labeling-1 and labeling-2 achieve the same performance which outperforms that of labeling-3 by considering the first bit of the QPSK symbol, and labeling-2 and labeling-3 achieve the same performance which outperforms that of labeling-1 by considering the second bit of the QPSK symbol. Thus, labeling-2 is optimal by considering both bits. Denote $\lambda_2 = d_2'/d_1'$, we have ${d_2'}^2 + {d_1'}^2 = 1$.

We mainly consider four flow information exchange, including two flows between A and R and two flows between A and B. The BER of each flow is defined as BER_{ar}, BER_{ra}, BER_{ab} and BER_{ba}, respectively. The objective is to maximize the weighted sum throughput, which is equivalent to minimizing the weighted BERs given by

$$\min_{\lambda_2} \; w_1\text{BER}_{ar} + w_2\text{BER}_{ra} + w_3\text{BER}_{ab} + w_4\text{BER}_{ba}, \tag{6}$$

where the weight coefficient, w_i, $i \in \{1, 2, 3, 4\}$, refers to the data importance, which is proportional to the importance of the corresponding data.

In this paper, we consider four flows with the same importance, and w_i equals the number of bits contained in symbol S_{jk}, where S_{jk} is the symbol from node j targeting to node k. For example, $w_i = 1$ in QPSK-BPSK H-PNC.

C. 8QAM-BPSK H-PNC

In this subsection, we present the 8QAM-BPSK H-PNC design. For 8QAM-BPSK H-PNC, there are two cases according to different demands of S_{ar}: case 1, source A transmits two units of data to relay R, and one unit to source B, i.e., S_{ar} consists of 2 bits and S_{ab} consists of 1 bit; case 2, source A transmits one unit of data to relay R, and two units to source B. The designs of these two cases are discussed in the following. Note that the designs for these two cases can be combined to support the non-integer data exchange ratio.

1) Case 1: The transmit constellation at source A in the MA stage and the broadcast constellation at relay R in the BC stage are shown in Figs. 5(a) and 5(b), labeled as constellation-1 and constellation-2, respectively. Constellation-1 and constellation-2 can be considered as 4/8-QAM and 2/8-QAM hierarchical constellations, respectively.[2] Note that to apply other 8QAM

[2]The prototypes of constellation-1 and constellation-2 are from two typical rectangular 8QAM constellations, i.e., $d_1 = 0$ for constellation-1 and $d_1' = \frac{d_2'}{2}$ for constellation-2.

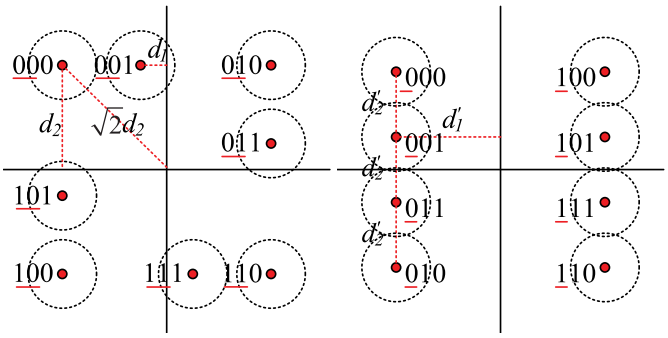

(a) Constellation-1. (b) Constellation-2.

Fig. 5. Constellations for 8QAM-BPSK H-PNC.

constellaion variants is also possible. However, the rectangular constellations as shown in Fig. 5 can be easily transmitted as PAM signals and can also be demodulated easily. Thus, they are studied in our work. In Fig. 5(a), the eight red points are the transmit constellation points, and the circles stand for the BPSK circles on the received constellation map at the relay. The first two bits of each symbol underlined is S_{ar}, and the left one bit is S_{ab}. The bit-symbol labeling criterion is similar to that discussed in QPSK-BPSK H-PNC in Subsection IV-B.1, i.e., symbols with the same S_{ar} are grouped, and symbols with the same S_{ab} are separated. For example, symbols 000 and 001 are grouped as they have the same $S_{ar} = 00$, and different S_{ar} are separated and positioned in Gray mapping; after positioning symbols 000 and 001 clockwise, the neighboring symbol of 001 is 010 instead of 011 to minimize BER_r at relay R in the mapping process, similar to that shown in Fig. 4. Define the coordinates of symbols 001 and 000 as $-d_1 + d_2 j$ and $-d_2 + d_2 j$, respectively. We have $d_1^2 + 3d_2^2 = 2$ with the average symbol energy constraint $E_s = 1$. Similar to (5), we obtain the optimal d_1 and d_2 by

$$\min_{d_1, d_2} \; 2 \cdot \text{BER}_r + \text{BER}_{ar}, \tag{7}$$

where coefficient 2 denotes that one incorrect estimation of S_{ar} may cause 1 bit error due to Gray mapping, and one incorrect estimation of S_n may cause 2 bit errors in the final demodulation of S_{ab} and S_{ba}.

The eight red points in Fig. 5(b) show the constellation points of the broadcast constellation at relay R. The first bit of each symbol underlined is the network-coded symbol S_n, and the left two bits are the superimposed bits S_{ra}. S_n is modulated in the base layer to guarantee the performance of the information exchange between source A and source B; S_{ra} is modulated in the enhancement layer in Gray mapping. Symbols starting with the same S_n are positioned with equal intervals to guarantee that different QPSK symbols S_{ra} have the similar error performance. We have energy constraint $4{d_1'}^2 + 5{d_2'}^2 = 4$. The optimal d_1' and d_2' are obtained according to (6). For higher-order modulation H-PNC, the same estimation approaches introduced in Section V can be used but with more complexities. In this work, their optimal constellation settings are obtained by the searching algorithm summarized as follows:

1) For the transmit constellation at source A, find a 4/8QAM prototype (constellation-1) and optimize the bit-symbol labeling according to the bit-symbol labeling criterion introduced in Subsection IV-B1.
2) Minimize (7) by exhaustively searching d_1 and d_2 with the energy constraint $d_1^2 + 3d_2^2 = 2$.
3) For the broadcast constellation at relay R, find a 2/8QAM prototype (constellation-2) and optimize the bit-symbol labeling in priority of the network-coded symbol.
4) Minimize (6) by exhaustively searching d_1' and d_2' with the energy constraint $4{d_1'}^2 + 5{d_2'}^2 = 4$.

2) Case 2: For the bit-symbol labeling, both the transmit constellation at source A in the MA stage, and the broadcast constellation at relay R in the BC stage use the 2/8-QAM constellation-2 as shown in Fig. 5(b). For the transmit constellation at source A, S_{ar} is modulated as the first bit of each symbol, and S_{ab} are the left two bits modulated in Gray mapping with equal intervals. Equal interval design tries to guarantee different BPSK circles of the received constellation map at relay R would have larger Euclidean distance on average. Due to the bottleneck link L_{br} which can support BPSK only given the BER threshold, two slots in the BC stage are needed to broadcast the network-coded symbol which is a QPSK symbol. In each BC slot, each bit of S_n is broadcast with the hierarchical constellation as shown in Fig. 5(b). The optimal constellation setting for the transmission constellation at source A is obtained by

$$\min_{d_1', d_2'} \; 3 \cdot \text{BER}_r + \text{BER}_{ar}, \tag{8}$$

where coefficient 3 denotes that one incorrect estimation of S_{ar} may cause 1 bit error, and one incorrect estimation of S_n may cause 3 end-to-end bits in error including 2 bits of S_{ab} and 1 bit of S_{ba}, as sources A and B cannot recover the correct information from an erroneous network-coded symbol. The optimal constellation setting of the broadcast constellation at relay R is obtained according to (6).

For case 2, adaptive mapping functions can be designed, i.e., the relay can select the optimal mapping function according to two source-relay channel conditions. When γ is small enough,[3] the optimal mapping functions are summarized in Table I. Relay R estimates two source-relay channel conditions, and obtains θ, and then selects the optimal mapping functions by looking up Table I. For example, when $\theta \in (0, \pi)$, the optimal mapping function $\mathcal{C}_1$ is selected. If the estimations $\hat{S}_{ab} = 00$ and $\hat{S}_{ba} = 0$, relay R obtains $S_n = \mathcal{C}_1(\hat{S}_{ab}, \hat{S}_{ba}) = \mathcal{C}_1(00, 0) = 00$ according to Table I. Please refer to [5], [21], and [22] for more details about the adaptive mapping design.

Note that, for both of 8QAM-BPSK H-PNC cases, in the BC stage, relay R can also superimpose one bit of S_{ra} instead of two bits on the network-coded symbol S_n to constitute a QPSK symbol instead of using 8QAM. The broadcast

[3] γ may be larger due to the deep channel fading, which will result in a large BER_r due to the overlapping of the BPSK circles in Fig. 5(b). Thus, in order to guarantee the end-to-end BER, transmissions should be avoided in these deep fading time slots using opportunistic scheduling solutions such as the Proportionally Fair Scheduling (PFS) used in the cellular systems, which is beyond the scope of this paper.

TABLE I
ADAPTIVE MAPPING FUNCTIONS

	$(00,0)$	$(01,0)$	$(11,0)$	$(10,0)$	$(00,1)$	$(01,1)$	$(11,1)$	$(10,1)$
$\mathcal{C}_1$, $\theta \in (0,\pi)$	00	01	11	10	01	11	10	00
$\mathcal{C}_2$, $\theta \in (\pi,2\pi)$	00	01	11	10	10	00	01	11

constellation can select the constellation as shown in Fig. 3(b). In this way, a better BER performance can be achieved in the BC stage at the cost of a lower system throughput. We can see that the H-PNC application is flexible to support different kinds of data exchange requirements and BER thresholds.

D. H-PNC Generalization

Consider 2^mQAM-2^nQAM H-PNC under asymmetric TWRC, where 2^m-QAM and 2^n-QAM are applied by the sources A and B, respectively. Assume $m > n$ without loss of generality. Consider that source A wants to transmit k bits and $(m-k)$ bits to source B and relay R, respectively, where k is an integer and $k \in \{1, \cdots, m-1\}$. Source B wants to transmit n bits to source A. The constellation map applied by source A and source B is an $(m-k)/m$-QAM hierarchical modulation constellation map and the traditional 2^n-QAM constellation map, respectively. The network-coded symbol obtained at relay R has a modulation order of $\max(k,n)$ subject to the Latin square constraint. Relay R uses an n/m hierarchical modulation constellation map by $\lceil \frac{\max(n,k)}{n} \rceil$ slots to broadcast the $\max(k,n)$-bit network-coded symbol subject to the bottleneck link. In each slot, maximal $(m-n)$ bits targeting from relay R to source A can be superimposed on the n-bit base layer symbol.

In the MA stage, the received constellation map at relay R has 2^{m+n} constellation points, where 2^{m-k} constellation points for the data from source A to relay R, are explicitly demodulated achieving by the $(m-k)/m$-QAM hierarchical modulation constellation map, and the leftover 2^{n+k} constellation points are mapped to the $\max(n,k)$-bit network-coded symbol. In the BC stage, source B uses $\lceil \frac{\max(n,k)}{n} \rceil$ slots to obtain the $\max(n,k)$-bit network-coded symbol by demodulating the n-bit on the base layer in each slot and then obtains the target information from source A by applying the information transmitted by itself and the mapping function reversely. Source A demodulates all of the m bits in each slot, where $(m-n)$ bits on the enhancement layer are the information from relay R to source A, and the n bits on the base layer are the information of the network-coded symbol. Note that the Euclidean distance between the constellation points on the hierarchical modulation constellation maps can be designed similarly to the algorithms in Section IV-C3.

V. QPSK-BPSK H-PNC ERROR PERFORMANCE ANALYSIS

In this section, we use the techniques introduced in [38] and [39] and study the error performance of QPSK-BPSK H-PNC under AWGN and Rayleigh fading channels.[4]

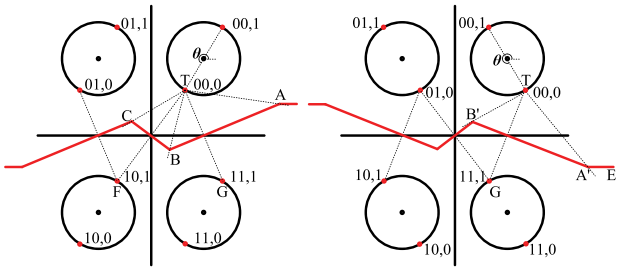

(a) $\theta \in (\pi, \frac{3\pi}{2})$. (b) $\theta \in (\frac{3\pi}{2}, 2\pi)$.

Fig. 6. Decision boundaries of BER_{ar}.

BER_{ar}, BER_{ra}, BER_{ab} and BER_{ba} are derived, receptively, so the problems of (5) and (6) can be directly solved.

A. Derivations of BER_{ar} and BER_{ra}

Given a modulation in any node, assume each symbol has an equivalent transmission probability. Denote $H_b/H_a = \gamma \exp(j\theta)$, where γ and θ are the amplitude ratio and phase shift difference between two source-relay channel gains, and θ has uniform distribution in $[0, 2\pi)$.[5] In Fig. 6, the decision boundaries of S_{ar} are shown by the red curves. The center of each circle is the target received symbol from source A. The four circles are obtained by superimposing two symbols from the sources with uniformed phase shift difference θ from $[0, 2\pi)$. The Euclidean distance between the original and each center of the circles is $|H_a|$, and the radius of each circle is $|H_b|$.

BER_{ar} denotes the bit transmission error rate from source A targeting to relay R in the MA stage. The error performance of BER_{ar} is obtained by considering symbol pair $(00,0)$ traversing the phase shift difference $\theta \in [0, 2\pi)$. The expected received constellation map at relay R is shown in Fig. 6, where the target symbol pair $(00,0)$ is labeled as T.

The coordinate of the target symbol pair $(00,0)$ is

$$[|H_a|\sqrt{\frac{1}{1+{\lambda_1}^2}} + |H_b|\cos(\theta)] + j[|H_a|\sqrt{\frac{{\lambda_1}^2}{1+{\lambda_1}^2}} + |H_b|\sin(\theta)],$$

where j is the imaginary unit.

For a target constellation point O as shown in Fig. 7, the error probability P_e that the received signal locates in the shadowed region R due to the Gaussian noise with a variance of $2\sigma^2$ can be calculated by

$$P_e = \frac{1}{2\pi}\int_0^{\theta_1} \exp\left(-\frac{L^2}{2\sigma^2 \sin^2(\theta' + \theta_2)}\right) \mathrm{d}\theta', \qquad (9)$$

[4]It is challenging to systematically characterize the decision boundaries for higher-order modulation H-PNC due to the complexity of the received constellation map at the relay. However, the steps to analyze their performance are similar to the approach presented here.

[5]If in the future, more accurate synchronization can be achieved so the range of θ can be reduced, the performance gain of H-PNC can be even higher, while the analytical framework developed in this paper can still be applicable.

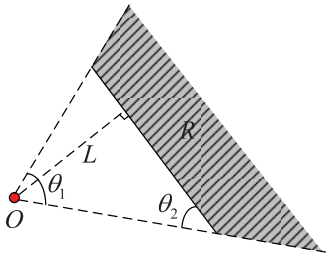

Fig. 7. Error probability.

where L is the Euclidean distance between O and the decision boundary, θ_1 and θ_2 are the radians labeled in Fig. 7. Please find the detailed proof in [38, eq. (9)].

Define $\Phi(\theta_1, \theta_2, L) = \frac{1}{2\pi}\int_0^{\theta_1} \exp(-\frac{L^2}{2\sigma^2 \sin^2(\theta'+\theta_2)})\ \mathrm{d}\theta'$. For $\theta \in (\pi, \frac{3\pi}{2})$ shown in Fig. 6(a), BER_{ar_1} can be estimated by

$$\mathrm{BER}_{ar_1} = \Phi(\angle\mathrm{BTA}, \angle\mathrm{ABT}, \frac{D_{TG}}{2}) + \Phi(\angle\mathrm{BTC}, \angle\mathrm{BCT}, \frac{D_{TF}}{2}), \quad (10)$$

where D_{ik} denotes the Euclidean distance between points i and k, and $\angle$ denotes the angle of union rad. The coordinates of A, B, G in Fig. 6(a) are given by

$$\begin{cases} G = [|H_a|\sqrt{\dfrac{1}{1+{\lambda_1}^2}} - |H_b|\cos(\theta)] \\ \qquad + j[-|H_a|\sqrt{\frac{{\lambda_1}^2}{1+{\lambda_1}^2}} - |H_b|\sin(\theta)], \\ B = [-|H_b|\cos(\theta)] \\ \qquad + j[|H_b|\cos(\theta)\frac{|H_a|\sqrt{1/(1+{\lambda_1}^2)}+|H_b|\cos(\theta)}{|H_a|\sqrt{{\lambda_1}^2/(1+{\lambda_1}^2)}+|H_b|\sin(\theta)}], \\ A = [\dfrac{|H_b|\sin\theta}{\tan(\theta-\pi/2)} + |H_a|\sqrt{\dfrac{1}{1+{\lambda_1}^2}}(1 - \dfrac{\lambda_1}{\tan(\theta-\pi/2)})] \\ \qquad - j[|H_b|\sin(\theta)]. \end{cases}$$

The coordinates of B and C are symmetric to the original point, so are that of T and F. Thus, coordinates of C and F can be easily obtained from B and T, so they are omitted due to the space limitation.

The BER_{ar_2} in the region $\theta \in [\frac{3\pi}{2}, 2\pi)$ shown in Fig. 6(b) can be estimated by

$$\mathrm{BER}_{ar_2} = \Phi(\angle\mathrm{B'TA'}, \angle\mathrm{A'B'T}, \frac{D_{TG}}{2}) + \Phi(\angle\mathrm{EA'T}, 0, |H_a|\sqrt{\frac{{\lambda_1}^2}{1+{\lambda_1}^2}}), \quad (11)$$

where $|H_a|\sqrt{\frac{{\lambda_1}^2}{1+{\lambda_1}^2}}$ is the Euclidean distance from T to the decision boundary A'E. The coordinates of A' and B' are

$$\begin{cases} A' = [\dfrac{|H_b|\sin(\theta)}{\tan(\theta-3\pi/2)} \\ \qquad + |H_a|\sqrt{\dfrac{1}{1+{\lambda_1}^2}}(\dfrac{\lambda_1}{\tan(\theta-3\pi/2)}+1)] + j[|H_b|\sin(\theta)], \\ B' = [|H_b|\cos(\theta)] \\ \qquad + j[|H_b|\cos(\theta)\dfrac{|H_a|\sqrt{1/(1+{\lambda_1}^2)} - |H_b|\cos(\theta)}{|H_a|\sqrt{{\lambda_1}^2/(1+{\lambda_1}^2)} + |H_b|\sin(\theta)}]. \end{cases}$$

For the region of $\theta \in [0, \pi)$, the Euclidean distance between the target T and the decision boundaries are much larger than that of the cases of $\theta \in [\pi, 2\pi)$, so the error rate can be neglected. Thus, BER_{ar} considering $\theta \in [0, 2\pi)$ can be expressed as

$$\begin{aligned} \mathrm{BER}_{ar} &= \Pr\{\theta \in (\pi, \frac{3\pi}{2})\}\mathrm{BER}_{ar_1} + \Pr\{\theta \in [\frac{3\pi}{2}, 2\pi)\}\mathrm{BER}_{ar_2} \\ &= \frac{\mathrm{BER}_{ar_1} + \mathrm{BER}_{ar_2}}{4}, \end{aligned} \quad (12)$$

where $\Pr\{.\}$ denotes the probability.

BER_{ra} denotes the error rate of the bits transmission from relay R to source A in the BC stage. Relay R uses a hierarchical constellation to broadcast the network-coded symbol S_n, which is superimposed by the symbol S_{ra} as the enhancement layer as shown in Fig. 3(b). Thus, BER_{ra} can be obtained by

$$\mathrm{BER}_{ra} = Q[\frac{|H_a|\sqrt{\frac{1}{1+{\lambda_2}^2}}}{\sigma}], \quad (13)$$

where $Q[.]$ is the Q function.

B. Derivations of BER_{ab} and BER_{ba}

The information exchange between sources A and B takes two-stage transmissions. BER_{ab} and BER_{ba} can be obtained similarly. BER_{ab} can be expressed as

$$\mathrm{BER}_{ab} = \mathrm{BER}_r(1 - \mathrm{BER}_{rb}) + (1 - \mathrm{BER}_r)\mathrm{BER}_{rb}, \quad (14)$$

where BER_{rb} denotes the error rate of broadcasting the network-coded symbol S_n from relay R to source B in the BC stage over link L_{br}.

1) BER_r: We first study how to estimate BER_r. Similar to the analysis to obtain BER_{ar}, we still consider the target symbol pair $(00, 0)$, and traverse the phase shift difference $\theta \in [0, 2\pi)$. The expected received constellation at relay R with different regions of θ are shown in Fig. 8.

We use Fig. 8(a) as an example to show how to calculate BER_r. The decision boundaries for the network-coded symbol S_n are shown by the red curves.[6] Denote the relay mapping error rate in the region $\theta \in (0, \frac{\pi}{4})$ as BER_{r1}, which can be expressed as

$$\begin{aligned} \mathrm{BER}_{r1} = \Phi(\angle\mathrm{JHT}, 0, |H_a|\sqrt{\frac{{\lambda_1}^2}{1+{\lambda_1}^2}}) \\ + \Phi(\pi - \angle\mathrm{TIK}, 0, |H_a|\sqrt{\frac{1}{1+{\lambda_1}^2}}) \\ + \Phi(\angle\mathrm{HTI}, \angle\mathrm{TIH}, |H_b|). \end{aligned} \quad (15)$$

Combining all the BER_{ri} of cases $i \in \{1, \cdots, 8\}$ results in the overall BER_r expressed as

$$\mathrm{BER}_r = \frac{1}{8}\sum_{i=1}^{8}\mathrm{BER}_{ri}. \quad (16)$$

[6]The red solid curves stand for the decision boundaries we calculated, and the red dashed curves stand for the decision boundaries with a typically much larger Euclidean distance from the target point T and they are neglected in our calculation.

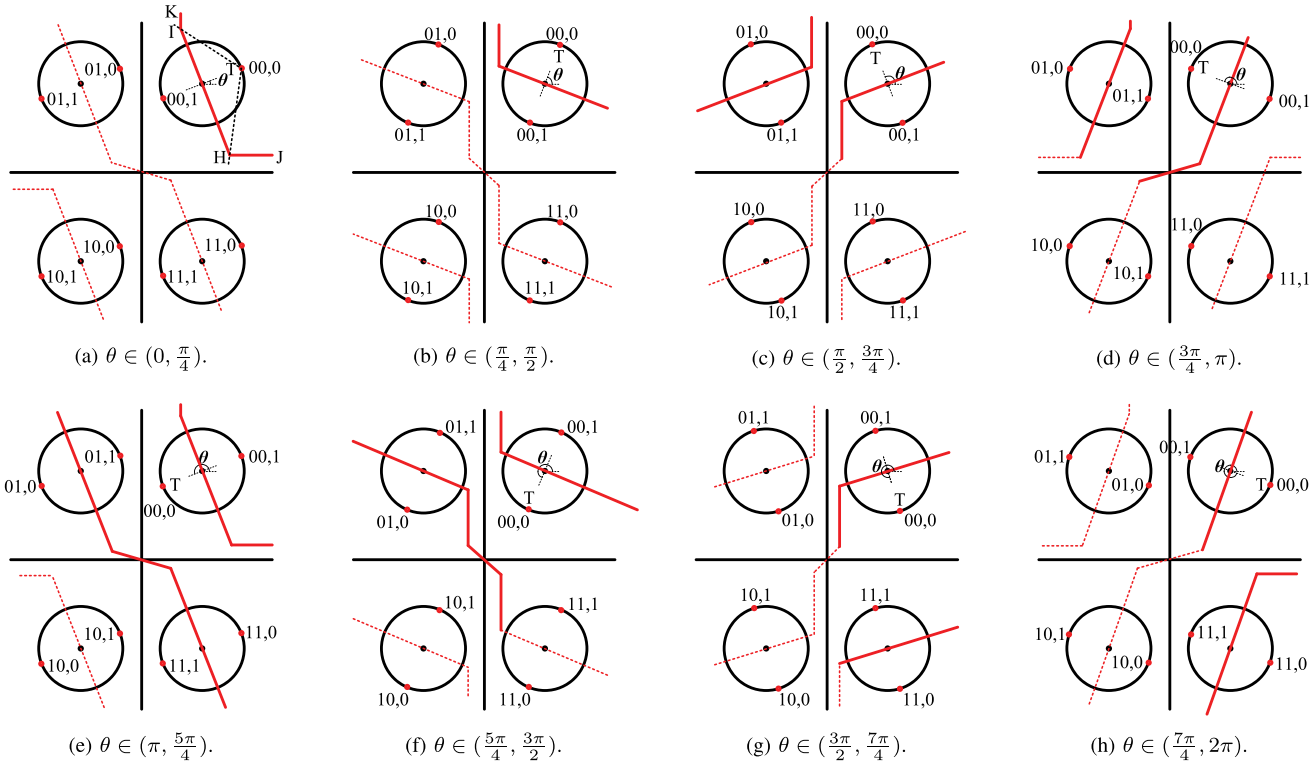

(a) $\theta \in (0, \frac{\pi}{4})$. (b) $\theta \in (\frac{\pi}{4}, \frac{\pi}{2})$. (c) $\theta \in (\frac{\pi}{2}, \frac{3\pi}{4})$. (d) $\theta \in (\frac{3\pi}{4}, \pi)$.

(e) $\theta \in (\pi, \frac{5\pi}{4})$. (f) $\theta \in (\frac{5\pi}{4}, \frac{3\pi}{2})$. (g) $\theta \in (\frac{3\pi}{2}, \frac{7\pi}{4})$. (h) $\theta \in (\frac{7\pi}{4}, 2\pi)$.

Fig. 8. Decision boundaries of BER_r.

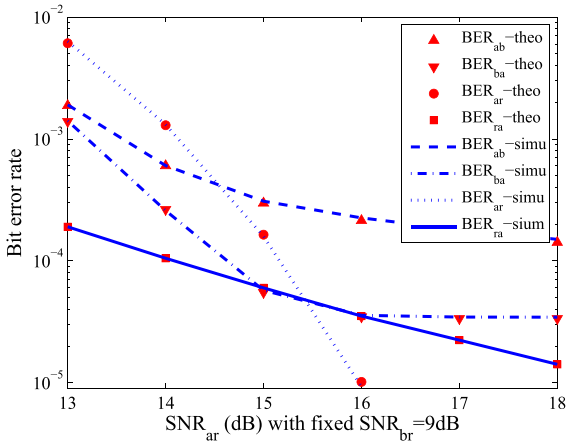

(a) AWGN channels.

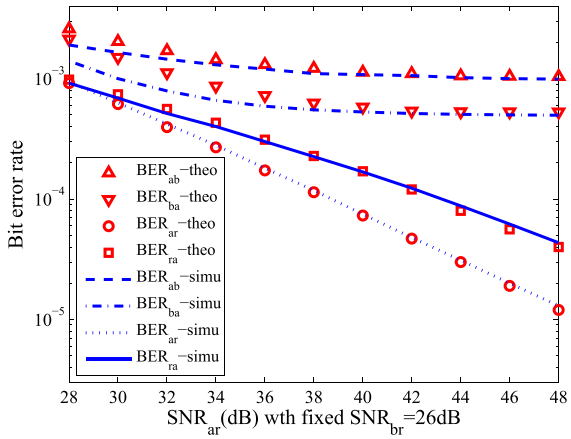

(b) Rayleigh fading channels.

Fig. 9. Theoretical results vs simulation results.

2) BER_{ab} and BER_{ba}: BER_{rb} denotes the BER of the base layer of the hierarchical constellation at relay R as shown in Fig. 3(b). We can easily obtain $\text{BER}_{rb} = Q[\frac{|H_b|\sqrt{\frac{\lambda_2{}^2}{1+\lambda_2{}^2}}}{\sigma}]$. Thus, substituting BER_{rb} into (14), we can obtain

$$\text{BER}_{ab} = \text{BER}_r(1 - Q[\frac{|H_b|\sqrt{\frac{\lambda_2{}^2}{1+\lambda_2{}^2}}}{\sigma}]) + (1 - \text{BER}_r) \times Q[\frac{|H_b|\sqrt{\frac{\lambda_2{}^2}{1+\lambda_2{}^2}}}{\sigma}]. \quad (17)$$

Similarly, BER_{ba} can be obtained by

$$\text{BER}_{ba} = \text{BER}_r(1 - Q[\frac{|H_a|\sqrt{\frac{\lambda_2{}^2}{1+\lambda_2{}^2}}}{\sigma}]) + (1 - \text{BER}_r) \times Q[\frac{|H_a|\sqrt{\frac{\lambda_2{}^2}{1+\lambda_2{}^2}}}{\sigma}]. \quad (18)$$

To summarize, BER_{ar}, BER_{ra}, BER_{ab} and BER_{ba} can be obtained by (12), (13), (17) and (18). Then the optimal λ_1 and λ_2 in (5) and (6) can be obtained. Fig. 9(a) shows that the theoretical results match the simulation results, where we

fix $\text{SNR}_{br} = 9$ dB and gradually increase SNR_{ar}(dB). When SNR_{ar} is larger enough, e.g., larger than 16 dB, the bit errors contribute to BER_{ba} is mainly caused by the signal superimposing in the MA stage subject to $\text{SNR}_{br} = 9$ dB, and the link L_{ar} is relatively good enough to forward the bits from relay R to source A with a large SNR_{ar}. Thus, when SNR_{ar} is large enough, BER_{ba} will converge to a value (about 3e-05 as shown in Fig. 9(a)) close to but higher than the BER of single-hop BPSK with SNR = 9dB (about 2e-05). Similarly, for BER_{ab}, roughly speaking it suffers from the bottleneck link L_{br} twice, which includes the signal superimposing in the multi-access stage and the forwarding from relay R to source B. Thus, when SNR_{ar} is large enough, BER_{ab} will converge to a value close but higher than twice of the single-hop BPSK BER.

C. Error Performance Analysis Under Rayleigh Fading Channels

We discuss the error performance analysis of QPSK-BPSK H-PNC under Rayleigh fading channels in this subsection. To obtain the exact BER of PNC-based under fading channels are quite challenging due to the complexity of the received constellation map at the relay specially when the higher-order modulations are applied by the sources. Denote the probability density function (PDF) of Rayleigh distribution as $f(x,\sigma) = \frac{x}{\sigma^2}\exp(\frac{-x^2}{2\sigma^2})$, with mean value $E(x) = \sigma\sqrt{\frac{\pi}{2}}$. Denote the PDF of channel gains $|H_a|$ and $|H_b|$ as $f(|H_a|,\sigma)$ and $f(|H_b|,\sigma)$, respectively.

The error performance of BER_{ar} can be estimated by considering the worst case when $\theta = \frac{\pi}{2}$ or $\frac{3\pi}{2}$ in Fig. 6, we have

$$\text{BER}_{ar} \approx \int_0^\infty \int_0^\infty f(|H_a|,\sigma) f(|H_b|,\sigma) \times Q[\frac{|H_a|\sqrt{\frac{\lambda_1^2}{1+\lambda_1^2}} - |H_b|}{\sigma}]\text{d}|H_a|\text{d}|H_b|. \quad (19)$$

From (13), the error performance of BER_{ra} can be obtained by

$$\text{BER}_{ra} = \int_0^\infty f(|H_a|,\sigma) Q[\frac{|H_a|\sqrt{\frac{1}{1+\lambda_1}}}{\sigma}]\text{d}|H_a|, \quad (20)$$

where $Q[.]$ is the Q-function.

From (15) and (16), BER_r can be approximated by

$$\text{BER}_r = \int_0^\infty f(|H_b|,\sigma) Q[\frac{|H_b|}{\sigma}]\text{d}|H_b|, \quad (21)$$

where only the closest decision boundaries in Fig. 8 are considered.

We can obtain BER_{ab} and BER_{ba} from (17) and (18) by replacing $Q[\frac{|H_a|\sqrt{\lambda_2^2/(1+\lambda_2^2)}}{\sigma}]$ and $Q[\frac{|H_b|\sqrt{\lambda_2^2/(1+\lambda_2^2)}}{\sigma}]$ with $\int_0^\infty f(|H_a|,\sigma) Q[\frac{|H_a|\sqrt{\lambda_2^2/(1+\lambda_2^2)}}{\sigma}]\text{d}|H_a|$ and $\int_0^\infty f(|H_b|,\sigma) Q[\frac{|H_b|\sqrt{\lambda_2^2/(1+\lambda_2^2)}}{\sigma}]\text{d}|H_b|$, respectively.

In Fig. 9(b), we compare the obtained theoretical results and the simulation results under Rayleigh fading channels.

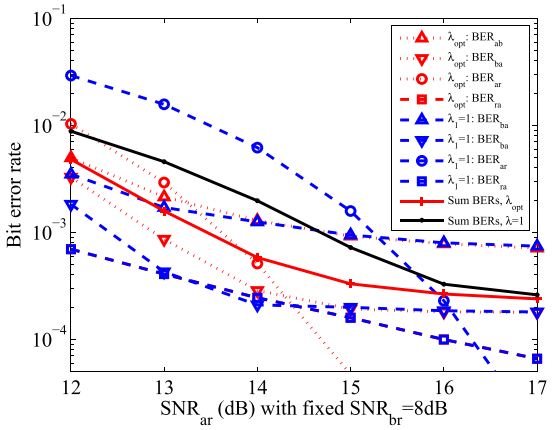

Fig. 10. QPSK-BPSK H-PNC with fixed $\text{SNR}_{br} = 8$ dB under AWGN channels.

Note that we set $\text{SNR}_{br} = 9$ dB and 26 dB under AWGN and Rayleigh fading channels to maintain the overall BER performance around 10e-03. It can be observed that the theoretical results match well with the simulation results for BER_{ar} and BER_{ra}. The small gap between the theoretical and simulation results for BER_{ab} and BER_{ba} are due to the approximation in (21), where only the closest Euclidean boundaries are considered. According to the algorithms in Section IV-C3, the values of λ_1 and λ_2 from 13 dB to 18 dB in Fig. 9(a) are 1.75, 1.77, 1.78, 1.78, 1.78, 1.78 and 1.47, 1.63, 1.81, 2.01, 2.24, 2.49, respectively. In Fig. 9(b), $\lambda_1 = 1.45$ and λ_2 are 1.4, 1.6, 1.8, 2.1, 2.4, 2.6, 2.8, 3.0, 3.2, 3.4, 3.6, respectively, from 28 dB to 48 dB with a 2 dB interval.

VI. Performance Evaluation

In this section, the performance of H-PNC is evaluated in under the asymmetric TWRC scenario. We studied a generalized physical-layer design without specifying any wireless communication system, and a slot duration equals the symbol duration. We first fix SNR_{br} and gradually increase SNR_{ar}, aiming to study how the source-relay channel conditions influence the constellation map design and the system performance under both AWGN and Rayleigh fading channels. Second, the throughput[7] and the throughput upper bound[8] performance of different H-PNC schemes are studied, aiming to study how to select H-PNC schemes with different channel conditions and various data exchange requirements. Let all the nodes transmit signals with the same symbol energy E_s, and the average received SNR of all links are proportional to the link distance to the power of the path-loss component ($\alpha = 3$). Phase shift difference θ is uniformly distributed between $[0, 2\pi)$.

A. BER Performance with Fixed SNR_{br}

The error performance of three H-PNC schemes under AWGN channels are shown in Figs. 10 and 11, where we fix $\text{SNR}_{br} = 8$ dB and gradually increase SNR_{ar}. Fig. 10 shows the error performance of QPSK-BPSK H-PNC.

[7]Throughput (bits/slot) is defined as the successfully received bits per slot by all the destinations.

[8]Throughput upper bound (bits/slot) is defined as the theoretical maximal throughput without considering the transmission bit errors.

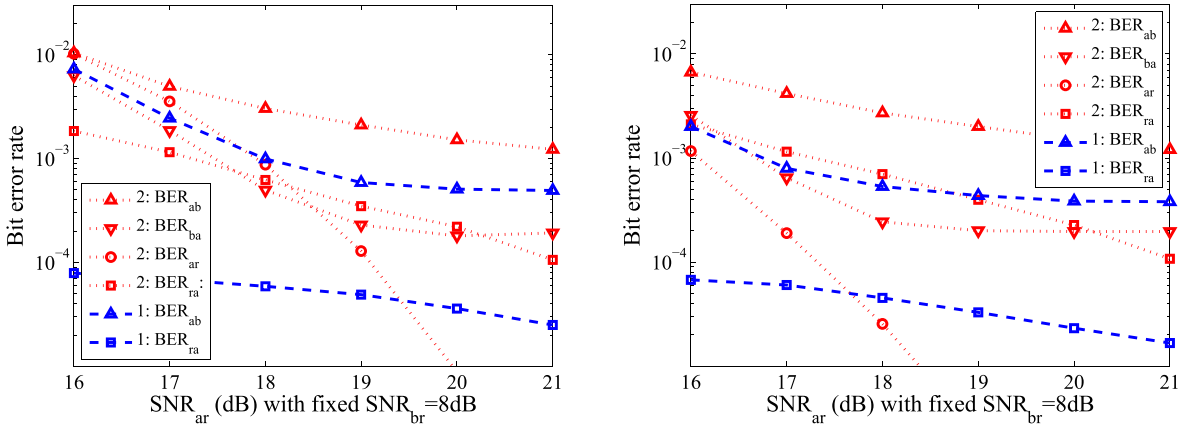

(a) 8QAM-BPSK H-PNC case 1. (b) 8QAM-BPSK H-PNC case 2.

Fig. 11. 8QAM-BPSK H-PNC with fixed $\mathrm{SNR}_{br} = 8$ dB under AWGN channels.

The red curves show the error performance with the optimal λ_1 and λ_2 obtained from (5) and (6), respectively. The blue curves are with the symmetric constellation setting in the MA stage, where $\lambda_1 = 1$ and λ_2 is set to the optimal value. We can observe that, without the hierarchical constellation design in the MA stage, BER_{ar} is much worse than BER_r (BER_r overlaps with BER_{ba} and thus is omitted in Fig. 10), which implies the necessity of the hierarchical constellation design. Considering the red curves, given SNR_{br} and when SNR_{ar} is large, $\gamma = |H_b|/|H_a| = 10^{(\mathrm{SNR}_{br}(\mathrm{dB})-\mathrm{SNR}_{ar}(\mathrm{dB}))/20}$ is small. Thus, BER_r is dominated by the errors happened within one BPSK circle and the error probability over link L_{ar} in the BC stage can be ignored, and that is also the reason why BER_r overlaps with BER_{ba}. Thus, both BER_r and BER_{ba} converge to the error performance of the single hop BPSK error performance with SNR $= 8$ dB under AWGN channels. BER_{ar} and BER_{ra} reduce with the increase of SNR_{ar} monotonously. The solid red and solid black curves are the sum $\frac{\mathrm{BER}s}{4}$ (we divide the sum BERs by 4 in order to fit in the same figure) performance of QPSK-BPSK H-PNC with or without optimized constellation design, respectively, which demonstrated the performance gain of our design in terms of sum BERs.

Figs. 11(a) and 11(b) show the error performance of 8QAM-BPSK case 1 and case 2, respectively. The optimal constellation setting are applied for both the transmit constellation at source A and the broadcast constellation at relay R obtained from (5), (7) and (8). The red curves denote that two bits of S_{ra} are superimposed on S_n in the BC stage. The blue curves denote that one bit of S_{ra} is superimposed on S_n. For the case that one bit of S_{ra} is superimposed, BER_{ar} and BER_{ba} are omitted, because BER_{ar} is not affected and BER_{ba} overlaps with that of the case two bits of S_{ra} are superimposed. From the red curves in Figs. 11(a) and 11(b), we can find that, BER_{ab} has the worse error performance, because the information delivery from source A to source B is under the bottleneck link L_{br} twice. Superimposing only one bit of S_{ra} can improve BER_{ab} due to the constellation setting modified in the BC stage. However, the throughput will reduce accordingly. Thus, there is a tradeoff between the error performance and the throughput. How many bits are superimposed in the BC stage depends on the data exchange ratio and error rate requirements.

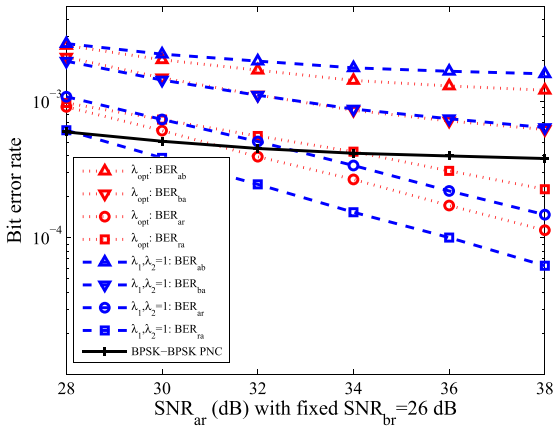

Fig. 12. QPSK-BPSK H-PNC with fixed $\mathrm{SNR}_{br} = 26$ dB under Rayleigh fading channels.

Figs. 12 and 13 show the error performance of three H-PNC schemes under Rayleigh fading channels, where we fix $\mathrm{SNR}_{br} = 26$ dB and gradually increase SNR_{ar}. In Fig. 12, when SNR_{ar} is large, BER_r is determined by the BPSK error performance with SNR $= 2$ dB under Rayleigh fading channels. Thus, BER_{ba} converges to BER_r as the error over L_{ar} is negligible, and BER_{ab} converges to twice BER_{ba} as the data from A to B are transmitted over the bottleneck link L_{br} twice. Figs. 13(a) and 13(b) show the 8QAM-BPSK H-PNC case 1 and case 2, respectively. The red curves are for the case that two bits of S_{ra} are superimposed in the BC stages, and the blue curves are for the case that only one bit of S_{ra} is superimposed. From the results, superimposing one bit of S_{ra} will improve BER_{ab} and BER_{ra} with a loss of throughput gain. The solid black curves are the end-to-end error performance, i.e., $\frac{\mathrm{BER}_{ab}+\mathrm{BER}_{ba}}{2}$, of BPSK-BPSK PNC. Given $\mathrm{SNR}_{br} =$ 26dB, when SNR_{ar} is large enough, the error performance of the network-coded symbol in the MA stage for QPSK-BPSK H-PNC and 8QAM-BPSK H-PNC is close to that of BPSK-BPSK PNC as the closest Euclidean distance on the

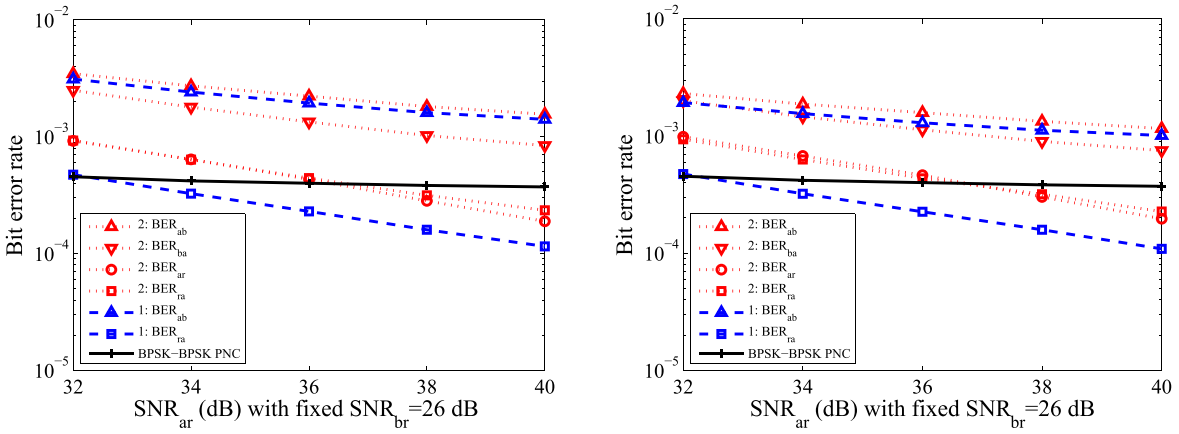

(a) 8QAM-BPSK H-PNC case 1.

(b) 8QAM-BPSK H-PNC case 2.

Fig. 13. 8QAM-BPSK H-PNC with fixed $\text{SNR}_{br} = 26$ dB under Rayleigh fading channels.

received constellation map at the relay, i.e., channel gain $|H_b|$, will determine the error performance of the network-coded symbol. For the end-to-end BER performance, BPSK-BPSK PNC outperforms QPSK-BPSK H-PNC as expected, given a lower-order modulation. However, the system throughput for BPSK-BPSK PNC, 1 bit/slot, is only half of that for QPSK-BPSK H-PNC. Combining both of the throughput and error performance, the system throughput upper bound of QPSK-BPSK H-PNC is much higher than that of BPSK-BPSK PNC.

B. Throughput Upper Bound Comparison

H-PNC achieves two bidirectional information exchange not only between the sources but also between the source with the better source-relay channel condition and the relay. The data exchange requirements between these two bidirectional information exchange impact on the system throughput of H-PNC. In this section, we study the impact of the data exchange requirements on the throughput upper bound. The throughput upper bounds of the proposed H-PNC, the traditional symmetric PNC[9] and the single-hop transmission are compared in Fig. 14. The throughput upper bound takes the summation of all the links, and is calculated with the unit of bits/slot, where the slots equals the symbol duration. If part of the bits cannot be transmitted by H-PNC or symmetric PNC scheme, the leftover bits are transmitted by the point-to-point transmissions hop-by-hop with the highest modulation-order supported by each hop. Denote the amount of data delivered by S_{ar}, S_{ra}, S_{ab} and S_{ba} as μ_{ar}, μ_{ra}, μ_{ab} and μ_{ba}, respectively. For QPSK-BPSK H-PNC and 8QAM-BPSK H-PNC case 1, which are both suitable to transmit data amount of $\mu_{ar} = \mu_{ra}$ and $\mu_{ab} = \mu_{ba}$. So is for symmetric PNC, which is suitable to exchange data amount $\mu_{ab} = \mu_{ba}$. Thus, denote $\beta_1 = \frac{\mu_{ar}}{\mu_{ab}}$, where $\mu_{ar} = \mu_{ra}$ and $\mu_{ab} = \mu_{ba}$. β_1 denotes the data amount between source A and relay R over that between sources A and B. For example, when $\beta_1 = 0$, H-PNC deteriorates to HePNC [22], and when β_1 goes to infinity, H-PNC deteriorates to the single-hop transmission from source A to relay R. Fig. 14(a) shows the throughput upper obund comparison of QPSK-BPSK H-PNC, BPSK-BPSK PNC and the single hop transmission. We can observe that QPSK-BPSK H-PNC is most suitable to support the data exchange ratio $\beta_1 = 1$, where totally 4 bits can be delivered in 2 slots. The maximum throughput upper bound gain compared with BPSK-BPSK PNC is 50%. For BPSK-BPSK PNC and the single hop transmission, the throughput upper bound increase with the increase of β_1. In Fig. 14(b), 8QAM-BPSK H-PNC case 1 achieves the highest throughput upper bound when $\beta_1 = 2$, where totally 6 bits can be delivered by 2 slots. The maximum throughput upper bound gain compared with BPSK-BPSK PNC is 66.7%.

For 8QAM-BPSK H-PNC case 2, the data exchange ratio between source A and B, and that between source A and relay R, is asymmetric. We denote $\beta_2 = \mu_{ar}/\mu_{ba}$ with $\mu_{ab} = 2\mu_{ba}$ and $\mu_{ra} = 2\mu_{ar}$.[10] In Fig. 14(c), the throughput upper bounds of three transmission schemes increase with the increase of β_2, and finally converges to 3 bits/slot, i.e., the majority bits are transmitted over link L_{ar} by 8QAM. When $\beta_2 = 1$, the maximum throughput upper bound gain compared with BPSK-BPSK PNC is 44%.

C. Discussion on H-PNC Scheme Selection.

In this subsection, we discuss the guide of H-PNC scheme selection. In Fig. 15, by fixing $\text{SNR}_{br} = 26$ dB and adjusting SNR_{ar} in a large range from 28 dB to 40dB, the throughput performance under Rayleigh fading channels by selecting different H-PNC schemes can be easily compared. We consider that one block contains 256 bits, and a block is successfully received if all bits are correctly received; otherwise, the block is dropped and the bis in the erroneous block are not counted in the throughput. Figs. 15(a), 15(b), 15(c) and 15(d) compare the throughput over different flows given source-relay channels by selecting different H-PNC schemes.

[9]Only BPSK-BPSK PNC can be applied as the symmetric PNC, due to that the bottleneck link L_{br} can only support BPSK.

[10]Note that, up to 2 bit of S_{ra} can be superimposed, which cause more asymmetric but a higher throughput gain. For a fair comparison purpose, Fig. 14(c) only considers 1 bit of S_{ra} is superimposed.

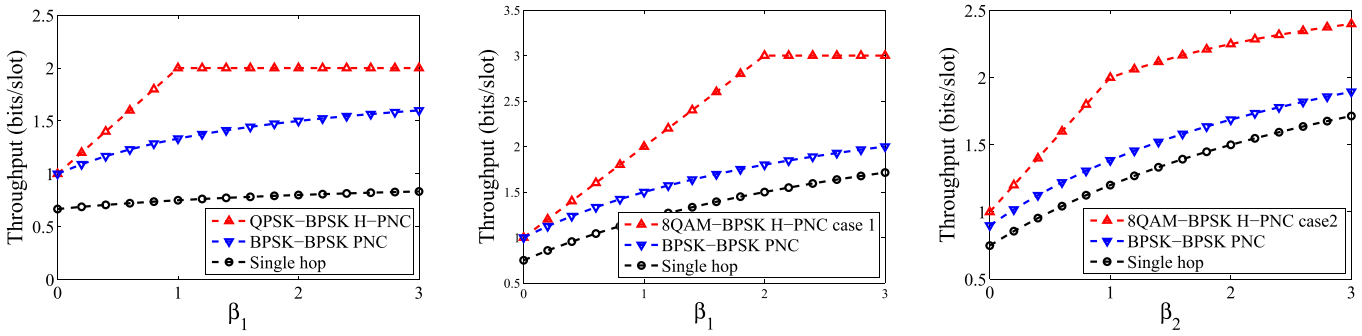

(a) QPSK-BPSK H-PNC. (b) 8QAM-BPSK H-PNC case 1. (c) 8QAM-BPSK H-PNC case 2.

Fig. 14. Throughput upper bounds of different transmission schemes.

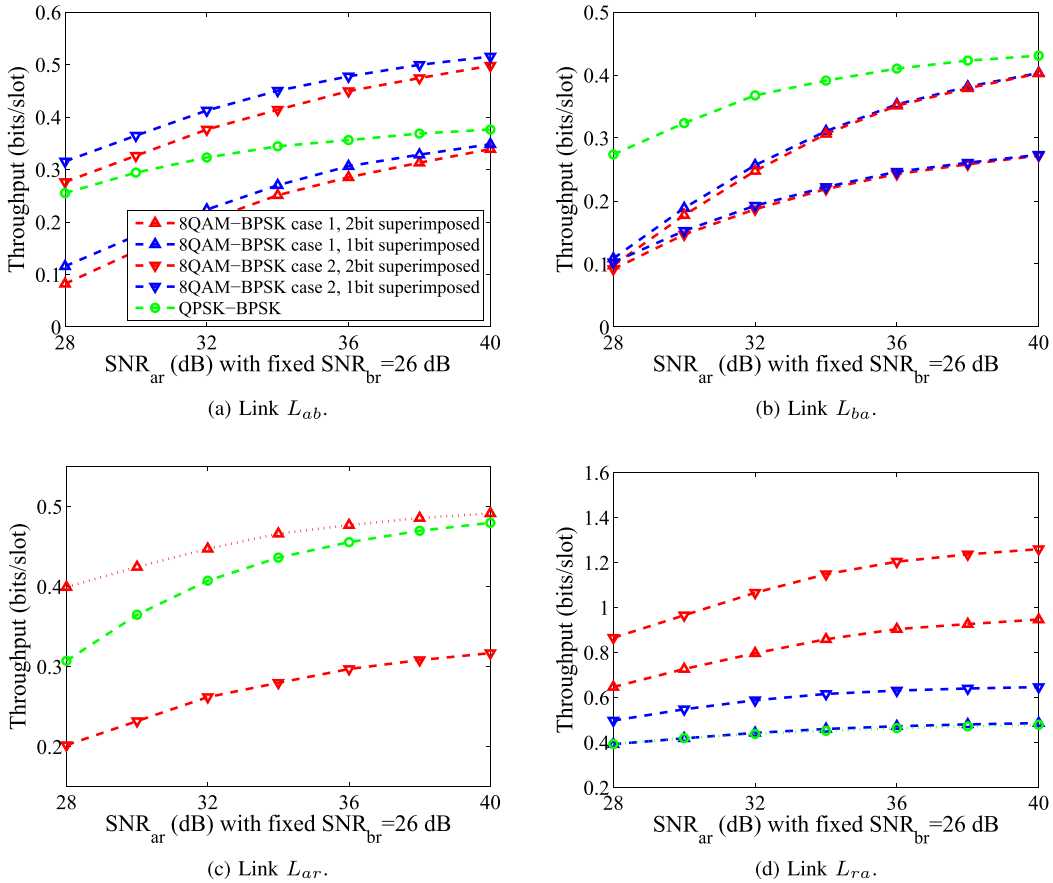

(a) Link L_{ab}. (b) Link L_{ba}.

(c) Link L_{ar}. (d) Link L_{ra}.

Fig. 15. Throughput under Rayleigh fading channels.

In Fig. 16, we compare the sum throughput (bits/slot) by different H-PNC schemes given two source-relay channels. The sum throughput adds up the throughput in each flow. In Fig. 16, 8QAM-BPSK H-PNC design with superimposing 2 bits in the BC stage achieves a higher sum throughput, as more bits from relay R to source A are delivered in the BC stage. When SNR_{ar} is low, e.g., from 28 dB to 40 dB, QPSK-BPSK H-PNC outperforms 8QAM-BPSK H-PNC superimposing 1 bit in the BC stage as the channel conditions are not sufficient to support the higher-order modulation. When SNR_{ar} is sufficiently high, QPSK-BPSK H-PNC and 8QAM-BPSK H-PNC case 1 (superimposing 1 bit in the BC stage) have similar sum throughput performance, as their theoretical sum throughput upper bounds are both 2 bits/slot. 8QAM-BPSK H-PNC case 2 (superimposing 1 bit in the BC stage) outperforms the previous two schemes slightly as its theoretical sum throughput upper bound is 2.5 bits/slot.

We should select the suitable H-PNC scheme by jointly considering the data exchange requirements among sources A and B and source A and relay R, two source-relay channel conditions and the BER requirement of each flow. For example, if sources A and B, and source A and the selected relay R exchange the same amount of data, QPSK-BPSK H-PNC is suggested and we can observe the throughput performance under different two source-relay channel conditions in Fig. 15. QPSK-BPSK H-PNC achieves the best

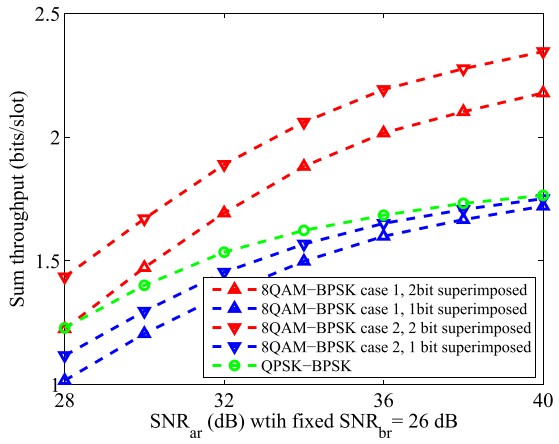

Fig. 16. Sum throughput comparison under Rayleigh fading channels.

data rate for flow from B to A compared to 8QAM-BPSK H-PNC as shown in Fig. 15(b). However, it achieves a relatively lower data rate for flow R to A as shown in Fig. 15(d). 8QAM-BPSK H-PNC achieves better BER_{ar} compared to QPSK-BPSK H-PNC as shown in Fig. 15(c), but relatively a lower data rate for flow from A to B as shown in Fig. 15(a). Thus, there is a tradeoff to select and configure H-PNC.

VII. Conclusion

In this paper, a new relaying scheme, H-PNC, has been proposed. Under the asymmetric TWRC scenario, the designs of heterogeneous modulation PNC and symmetric PNC cannot fully utilize the channel of the source-relay with a better channel condition in the BC stage and the MA stage, respectively. By combining the hierarchical modulation and heterogeneous modulation PNC designs, H-PNC achieves the data exchange not only between two sources, but also between the relay node and the source with a relatively better source-relay channel condition. H-PNC outperforms the heterogeneous modulation PNC and symmetric PNC in terms of the system throughput. We have presented three H-PNC schemes, including QPSK-BPSK and two cases of 8QAM-BPSK H-PNC, where the designs of the bit-symbol labeling, the hierarchical modulation constellations and the mapping functions are jointly optimized. We also concluded a generalized H-PNC design criterion. We have provided the error performance analysis of QPSK-BPSK H-PNC under both AWGN and Rayleigh fading channels, where the amplitude ratio and the phase shift difference between the channel gains of the source-relay links are carefully addressed. Extensive simulations have been conducted to evaluate the system performance in terms of end-to-end BER, throughput and throughput upper bound. H-PNC can achieve substantial performance gains comparing to heterogeneous modulation PNC and symmetric PNC under asymmetric TWRC.

Given the promises of this direction, there are many issues to be further considered in the future work. For the higher-order modulation pair H-PNC, due to the complexity of the superimposing constellation map at the relay, how to generalize the constellation design and bit-symbol labeling for arbitrary higher-order modulation pairs is worth further research. In the multi-user multi-relay PNC scenario, the system groups two sources and one relay to construct a PNC-group. The H-PNC technique introduced in this paper can be applied in each PNC-group. However, different from the pure multi-user PNC system, the grouping and scheduling algorithm in the multi-user H-PNC scenario should further consider the data amount exchanged between the relay and the BC, which is an interesting topic for further research. Opportunistic scheduling is a link-layer solution, which considers the instantaneous PHY layer channel conditions to schedule users with better channel conditions to transmit, aiming to achieve multi-user diversity gain. H-PNC is a PHY-layer design, which considers the network topology and channel conditions of links between three nodes to achieve overall better end-to-end performance. These two solutions are orthogonal and can be applied together in a practical system. How to apply and optimize both is an interesting further research issue.

References

[1] H. Zhang, L. Zheng, and L. Cai, "PiPNC: Piggybacking physical layer network coding for multihop wireless networks," in *Proc. IEEE ICC*, Jun. 2015, pp. 6211–6216.
[2] S. Zhang, S. C. Liew, and P. P. Lam, "Hot topic: Physical-layer network coding," in *Proc. ACM MOBICOM*, 2006, pp. 358–365.
[3] P. Popovski and H. Yomo, "The anti-packets can increase the achievable throughput of a wireless multi-hop network," in *Proc. IEEE ICC*, Jun. 2006, pp. 3885–3890.
[4] S. C. Liew, S. Zhang, and L. Lu, "Physical-layer network coding: Tutorial, survey, and beyond," *Phys. Commun.*, vol. 6, pp. 4–42, Mar. 2013.
[5] T. Koike-Akino, P. Popovski, and V. Tarokh, "Optimized constellations for two-way wireless relaying with physical network coding," *IEEE J. Sel. Areas Commun.*, vol. 27, no. 5, pp. 773–787, Jun. 2009.
[6] V. Muralidharan, V. Namboodiri, and B. Rajan, "Wireless network-coded bidirectional relaying using Latin squares for M-PSK modulation," *IEEE Trans. Inf. Theory*, vol. 59, no. 10, pp. 6683–6711, Oct. 2013.
[7] R. H. Louie, Y. Li, and B. Vucetic, "Practical physical layer network coding for two-way relay channels: Performance analysis and comparison," *IEEE Trans. Wireless Commun.*, vol. 9, no. 2, pp. 764–777, Feb. 2010.
[8] Z. Faraji-Dana and P. Mitran, "On non-binary constellations for channel-coded physical-layer network coding," *IEEE Trans. Wireless Commun.*, vol. 12, no. 1, pp. 312–319, Jan. 2013.
[9] P. C. Wang, Y. C. Huang, and K. R. Narayanan, "Asynchronous physical-layer network coding with quasi-cyclic codes," *IEEE J. Sel. Areas Commun.*, vol. 33, no. 2, pp. 309–322, Feb. 2015.
[10] Q. Yang and S. C. Liew, "Asynchronous convolutional-coded physical-layer network coding," *IEEE Trans. Wireless Commun.*, vol. 14, no. 3, pp. 1380–1395, Mar. 2015.
[11] T. Huang, T. Yang, J. Yuan, and I. Land, "Design of irregular repeat-accumulate coded physical-layer network coding for Gaussian two-way relay channels," *IEEE Trans. Commun.*, vol. 61, no. 3, pp. 897–909, Mar. 2013.
[12] L. Yang, T. Yang, J. Yuan, and J. An, "Achieving the near-capacity of two-way relay channels with modulation-coded physical-layer network coding," *IEEE Trans. Wireless Commun.*, vol. 14, no. 9, pp. 5225–5239, Sep. 2015.
[13] N. Lee and R. W. Heath, "Space–time physical-layer network coding," *IEEE J. Sel. Areas Commun.*, vol. 33, no. 2, pp. 323–336, Feb. 2015.
[14] A. K. Tanc, T. M. Duman, and C. Tepedelenlioglu, "Design of LDPC codes for two-way relay systems with physical-layer network coding," *IEEE Commun. Lett.*, vol. 17, no. 12, pp. 2356–2359, Dec. 2013.
[15] J. He and S. C. Liew, "Building blocks of physical-layer network coding," *IEEE Trans. Wireless Commun.*, vol. 14, no. 5, pp. 2711–2728, May 2015.
[16] L. Bo, W. Gang, P. H. J. Chong, Y. Hongjuan, Y. Guan, and S. Xuejun, "Performance of physical-layer network coding in asymmetric two-way relay channels," *Commun., China*, vol. 10, no. 10, pp. 65–73, Oct. 2013.
[17] T. Koike-Akino, P. Popovski, and V. Tarokh, "Adaptive modulation and network coding with optimized precoding in two-way relaying," in *Proc. IEEE Globecom*, Dec. 2009, pp. 1–6.

[18] Z. Chen, H. Liu, and W. Wang, "A novel decoding-and-forward scheme with joint modulation for two-way relay channel," *IEEE Commun. Lett.*, vol. 14, no. 12, pp. 1149–1151, Dec. 2010.
[19] Z. Chen, H. Liu, and W. Wang, "On the optimization of decode-and-forward schemes for two-way asymmetric relaying," in *Proc. IEEE ICC*, Jun. 2011, pp. 1–5.
[20] Z. Chen and H. Liu, "Spectrum-efficient coded modulation design for two-way relay channels," *IEEE J. Sel. Areas Commun.*, vol. 32, no. 2, pp. 251–263, Feb. 2014.
[21] H. Zhang, L. Zheng, and L. Cai, "HePNC: Design of physical layer network coding with heterogeneous modulations," in *Proc. IEEE Globecom*, Dec. 2014, pp. 2684–2689.
[22] H. Zhang, L. Zheng, and L. Cai, "Design and analysis of heterogeneous physical layer network coding," *IEEE Trans. Wireless Commun.*, vol. 15, no. 4, pp. 2484–2497, Apr. 2016.
[23] L. Shi, S. C. Liew, and L. Lu, "On the subtleties of q-PAM linear physical-layer network coding," *IEEE Trans. Inf. Theory*, vol. 62, no. 5, pp. 2520–2544, May 2016.
[24] B. Rankov and A. Wittneben, "Achievable rate regions for the two-way relay channel," in *Proc. IEEE Int. Symp. Inf. Theory*, Jul. 2006, pp. 1668—1672.
[25] T. J. Oechtering, C. Schnurr, I. Bjelakovic, and H. Boche, "Broadcast capacity region of two-phase bidirectional relaying," *IEEE Trans. Inf. Theory*, vol. 54, no. 1, pp. 454–458, Jan. 2008.
[26] W. Nam, S.-Y. Chung, and Y. H. Lee, "Capacity of the Gaussian two-way relay channel to within $\frac{1}{2}$ bit," *IEEE Trans. Inf. Theory*, vol. 56, no. 11, pp. 5488–5494, Nov. 2010.
[27] L. Lu, L. You, and S. C. Liew, "Network-coded multiple access," *IEEE Trans. Mobile Comput.*, vol. 13, no. 12, pp. 2853–2869, Dec. 2014.
[28] Y. Fan, Y. Jiang, H. Zhu, and X. Shen, "PIE: Cooperative peer-to-peer information exchange in network coding enabled wireless networks," *IEEE Trans. Wireless Commun.*, vol. 9, no. 3, pp. 945–950, Mar. 2010.
[29] R. Ahlswede, N. Cai, S.-Y. R. Li, and R. W. Yeung, "Network information flow," *IEEE Trans. Inf. Theory*, vol. 46, no. 4, pp. 1204–1216, Jul. 2000.
[30] B. Rankov and A. Wittneben, "Spectral efficient protocols for half-duplex fading relay channels," *IEEE J. Sel. Areas Commun.*, vol. 25, no. 2, pp. 379–389, Feb. 2007.
[31] R. Zhang, "On achievable rates of two-path successive relaying," *IEEE Trans. Mobile Comput.*, vol. 57, no. 10, pp. 2914–2917, Dec. 2009.
[32] K. Ravindran, A. Thangaraj, and S. Bhashyam, "High SNR error analysis for bidirectional relaying with physical layer network coding," *IEEE Trans. Wireless Commun.*, vol. 65, no. 4, pp. 1536–1548, Apr. 2017.
[33] L. Cai, S. Xiang, Y. Luo, and J. Pan, "Scalable modulation for video transmission in wireless networks," *IEEE Trans. Veh. Technol.*, vol. 60, no. 9, pp. 4314–4323, Nov. 2011.
[34] Z. Yang, L. Cai, Y. Luo, and J. Pan, "Topology-aware modulation and error-correction coding for cooperative networks," *IEEE J. Sel. Areas Commun.*, vol. 30, no. 2, pp. 379–387, Feb. 2012.
[35] J. M. Park, S.-L. Kim, and J. Choi, "Hierarchically modulated network coding for asymmetric two-way relay systems," *IEEE Trans. Veh. Technol.*, vol. 59, no. 5, pp. 2179–2184, Jun. 2010.
[36] L. Lu, T. Wang, S. C. Liew, and S. Zhang, "Implementation of physical-layer network coding," in *Proc. IEEE ICC*, Jun. 2012, pp. 4734–4740.
[37] Y. Huang, S. Wang, Q. Song, L. Guo, and A. Jamalipour, "Synchronous physical-layer network coding: A feasibility study," *IEEE Trans. Wireless Commun.*, vol. 12, no. 8, pp. 4048–4057, Aug. 2013.
[38] J. W. Craig, "A new, simple and exact result for calculating the probability of error for two-dimensional signal constellations," in *Proc. IEEE MILCOM*, Nov. 1991, pp. 571–575.
[39] A. Y. C. Peng, S. Yousefi, and I. M. Kim, "On error analysis and distributed phase steering for wireless network coding over fading channels," *IEEE Trans. Wireless Commun.*, vol. 8, no. 11, pp. 5639–5649, Nov. 2009.

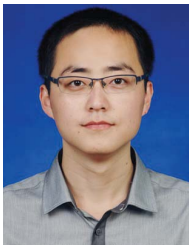

Haoyuan Zhang (S'14) received the B.S. and M.S. degrees from the Department of Electrical and Information Engineering, Harbin Institute of Technology, Harbin, China, in 2010 and 2012, respectively, and the Ph.D. degree from the Department of Electrical and Computer Engineering, University of Victoria, Victoria, BC, Canada, in 2017. His current research interests include channel error control coding, modulation optimizations, physical-layer network coding, and massive MIMO communications.

Lei Zheng (S'11) received the B.S. and M.S. degrees in electrical engineering from the Beijing University of Posts and Telecommunications, Beijing, China, in 2007 and 2010, respectively, and the Ph.D. degree from the University of Victoria, Victoria, BC, Canada, in 2015. His research interest is machine-to-machine networks, including medium access control protocol, radio resource allocation in wireless networks, and demand response control in smart grid.

Lin Cai (S'00–M'06–SM'10) received the M.A.Sc. and Ph.D. degrees in electrical and computer engineering from the University of Waterloo, Waterloo, Canada, in 2002 and 2005, respectively. Since 2005, she has been with the Department of Electrical and Computer Engineering, University of Victoria, where she is currently a Professor. Her research interests span several areas in communications and networking, with a focus on network protocol and architecture design supporting emerging multimedia traffic over wireless, mobile, ad hoc, and sensor networks. She was a recipient of NSERC Discovery Accelerator Supplement Grants in 2010 and 2015, respectively, and the Best Paper Awards of the IEEE ICC 2008 and the IEEE WCNC 2011. She has served as a TPC Symposium Co-Chair of the IEEE Globecom 2010 and Globecom 2013, an Associate Editor of the IEEE TRANSACTIONS ON WIRELESS COMMUNICATIONS, the IEEE TRANSACTIONS ON VEHICULAR TECHNOLOGY, the *EURASIP Journal on Wireless Communications and Networking*, the *International Journal of Sensor Networks*, and the *Journal of Communications and Networks*, and a Distinguished Lecturer of the IEEE VTS Society.